CRYSTAL GROWTH & DESIGN

Article

pubs.acs.org/crystal

Diversities of Coordination Geometry Around the Cu^{2+} Center in Bis(maleonitriledithiolato)metalate Complex Anions: Geometry Controlled by Varying the Alkyl Chain Length of Imidazolium Cations

Ravada Kishore and Samar K. Das*

School of Chemistry, University of Hyderabad, P.O. Central University, Hyderabad, 500046, India

Supporting Information

ABSTRACT: Six new ion-pair metal-bis(dithiolene) complexes with the formulas $[C_9H_{14}N_4][Cu(mnt)_2]$ (**1a**), $[C_{10}H_{16}N_4][Cu(mnt)_2]$ (**1b**), $[C_{11}H_{18}N_4][Cu(mnt)_2]$ (**1c**), $[C_{12}H_{20}N_4][Cu(mnt)_2]$ (**1d**), $[C_{13}H_{22}N_4][Cu(mnt)_2]$ (**1e**), and $[C_{14}H_{24}N_4][Cu(mnt)_2]$ (**1f**) have been synthesized starting from Cu(II) salt, Na_2mnt (disodium maleonitriledithiolate), and bromide salts of alkyl-bis(imidazolium) cations $[C_8H_{12}(CH_2)_nN_4Br_2]$ (n = 1−6, **a**−**f**). In this series of ion-pair compounds **1a**−**1f**, a common $[Cu(mnt)_2]^{2-}$ complex anion is associated with alkyl imidazolium cations of varied alkyl chain lengths. We have described a systematic study of deviation from square planar geometries (in terms of distortion) around the metal ion in customary square planar metal-dithiolene complexes. The distortion in the geometry around the metal ion can be explained on the basis of center of symmetry along C−H···Cu supramolecular interaction and unbalanced supramolecular interactions, such as S···H, N···H, and M···S type weak contacts. Dianionic copper(II) complexes **1a**−**1f** show an electronic absorption in the near-infrared (NIR) region, which has been attributed to the charge transfer transition from the highest occupied molecular orbital level of copper dithiolate anion $[Cu(mnt)_2]^{2-}$ to the lowest unoccupied molecular orbital level of alkyl imidazolium cation $[C_8H_{12}(CH_2)_nN_4]^{2+}$. All these compounds are unambiguously characterized by single crystal X-ray crystallography and further characterized by IR, ^{1}H NMR, electron spin resonance, LC/MS spectroscopic techniques, and electrochemical studies.

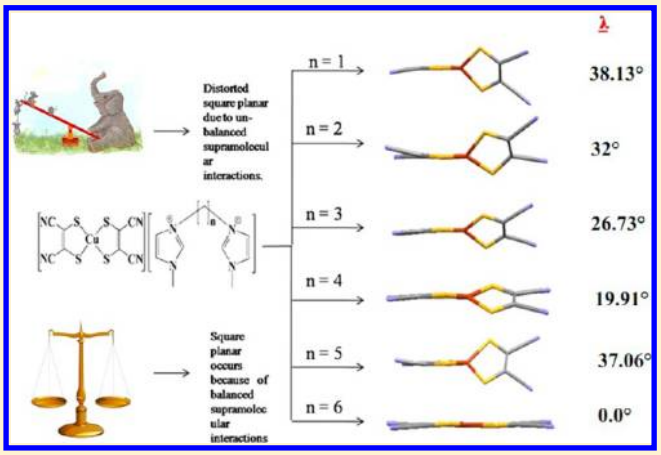

INTRODUCTION

Transition metal bis(dithiolene) complexes have attracted considerable research attention for more than three decades,[1−3] because of their brilliant redox behavior and favorable solid state interactions in their corresponding metal coordination complexes. Metal bis(1,2-dithiolene) complexes have been studied extensively in terms of their conducting, superconducting, nonlinear optical and magnetic behavior.[4] Ion-pair dithiolene complexes have also been used as near-IR dyes and in Q-switching laser studies.[4f] Planarity/nonplanarity of the metal-dithiolene complex moiety is one of the important factors to exhibit absorption in the near-IR region.[1f,5] Generally dithiolene ligands form square-planar transition-metal bis-(dithiolato) complexes;[6,7] some metal-dithiolene complexes show deviation from this planarity.[8,9] This deviation is usually caused by the constraints of the metal-chelate rings.[10] This sort of distortion is also found in metal−thiolato complex; for example, the asymmetric unit in the crystal structure of the complex $[Ni\{^iPr_2P(S)NP(S)Ph_2\}_2]$ consists of two independent molecules: one of them is square planar and the other one is distorted square planar.[11] This was explained by the orientation of methyl groups and the supramolecular interactions that involve the Ni···H−C hydrogen bond. The relevant square planar complex exhibits a center of symmetry along the Ni···H−C hydrogen bond with a bond distance of 2.607 Å, and in the distorted molecule, two different Ni···H−C (2.722, 2.734 Å) supramolecular interactions are present, which indicates the lack of a center of symmetry along Ni···H, resulting in distortion around the metal ion. This study suggests that the geometry around the metal ion is influenced by intramolecular hydrogen bonding interactions. Besides these asymmetric hydrogen bonding interactions, there are other factors that can influence the geometry around the metal ion; for example, varying the alkyl chain length of the associated ligand can cause distortion of a square planar geometry around a metal ion by varying metal−ligand bond lengths.[12] The presence of a bulky group can also influence the geometry around the metal ion, because packing of these bulky groups plays an important role.[13] In an iron-porphyrin system $FeTPP(N\text{-}MeIm)_2$ (TPP = tetrakis(*o*-pivalamidophenyl)-

Received: April 11, 2012
Revised: May 27, 2012

   dx.doi.org/10.1021/cg3004917 | *Cryst. Growth Des.* XXXX, XXX, XXX−XXX

Scheme 1. Synthetic Procedure of the Complexes

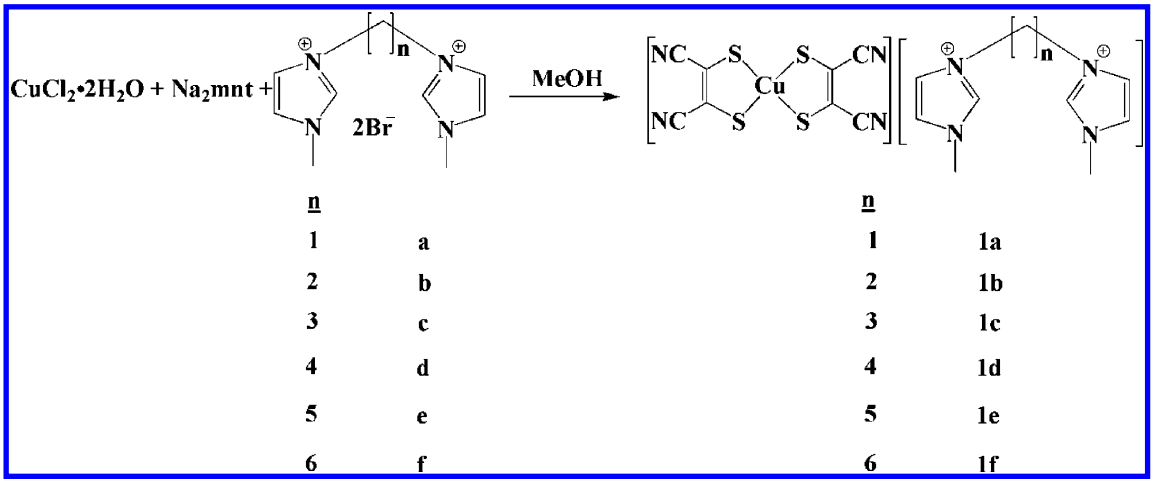

n		n	
1	a	1	1a
2	b	2	1b
3	c	3	1c
4	d	4	1d
5	e	5	1e
6	f	6	1f

porphyrins), when the bis-*N*-MeIm (*N*-methylimidazole) ligands, coordinated to iron, are replaced by bulky ligands DCHIm (1,5-dicyclohexylimidazole), the visible absorption bands are significantly red-shifted for the *αααββ* and *αβαβ* atropisomers of the relevant complex.[14] This shift has been explained on the basis of a change in porphyrin structure from a planar to a nonplanar conformation.[15] The blue copper sites of copper blue protein exhibit a number of characteristics that arise from distorted coordination geometries at the metal center.[16]

Thus the deviation of a square planar geometry around a metal ion can be caused by a number of factors that include center of symmetry along the M···H bond, increasing the chain of alkyl groups of the associated cation, the presence of bulky groups and the supramolecular interactions of the types N···H, S···H, M···H, and M···S weak contacts. The theme of the present work is how increasing length of the alkyl chain of the imidazolium cation affects the geometry of a square planar copper bis(dithiolato) complex anion in the solid state. We report here six new ion pair copper-bis(dithiolato) complexes $[C_8H_{12}(CH_2)_nN_4][Cu(mnt)_2]$ [n = 1−6, **1a−1f**] in which the counter cations are varied by increasing chain length of the cation retaining the same complex anion $[Cu(mnt)_2]^{2-}$ in all compounds **1a−1f**. The geometry around the metal ion can be tuned by supramolecular interactions of the complex anion with the surrounding organic cations in respective ion-pair complexes. The nonclassical M···H bonding interactions are observed in organometallic compounds,[17] and in ion-pair dithiolene complexes.[18] In their diffuse reflectance spectra, there is a trend (the shift of the absorption maxima) among these complexes **1a−1f**. More specifically, if the distortion angle between two SCuS planes[1f] (of the complex anion) is more, the band in near-IR region shifts toward a more low energy region. Thus, the more the distortion around the metal ion, the relevant absorption maximum shifts to a more red region. All compounds **1a−1f** have been characterized by routine elemental analysis, ^{1}H NMR, LC-MS, electron paramagnetic resonance (EPR) spectroscopy, and cyclic volatmmetry and finally characterized by single crystal X-ray diffraction.

EXPERIMENTAL DETAILS

Materials and Methods. All chemicals were purchased from commercial sources and used without further purification. Micro analytical (C, H, N) data were obtained with a FLASH EA 1112 Series CHNS Analyzer. The IR spectra (with KBr pellets) were recorded in the range of 400−4000 cm^{-1} on a JASCO FT/IR-5300, and NICOLET 380 FT-IR spectrometer. UV−vis spectra were recorded on a Cary 100 Bio UV−vis spectrophotometer. Diffuse reflectance and near-IR absorption spectra were recorded on a UV-3600 Shimadzu UV−vis-NIR spectrophotometer. The electron spin resonance (ESR) spectra were recorded on a (JEOL) JESFA200 ESR spectrometer. ^{1}H NMR spectra was recorded on Bruker DRX- 400 and 500 spectrometer using $Si(CH_3)_4$ (TMS) as an internal standard. Solution mass spectra (LC/MS) were obtained on a LCMS-2010A Shimadzu spectrometer. Powder X-ray diffraction patterns were recorded on a Bruker D8-Advance diffractometer using graphite monochromated $CuK_{\alpha1}$ (1.5406 Å) and $K_{\alpha2}$ (1.54439 Å) radiations. A Cypress model CS-1090/CS-1087 electroanalytical system was used for cyclic voltammetric experiments. The electrochemical experiments were measured in acetonitrile solvent containing $[Bu_4N][ClO_4]$ as a supporting electrolyte, using a conventional cell consisting of two platinum wires as working and counter electrodes and a Ag/AgCl electrode as a reference.

*Synthetic Procedures for Alkyl Imidazolium Derivatives (**a**−**f**) (see also Scheme 1).* Preparation of imidazolium derivates are modified from the literature procedure.[19] To the 1-methyl imidazole (2 mmol) solution of toluene (30 mL), 1,*n*-dibromo alkane (1 mmol) (n = 1−6) was added. This reaction mixture was refluxed for overnight and toluene was removed by rotary evaporator and the crude product was washed with *n*-hexane and air-dried and finally stored in the freezer for solidification.

*3,3′-Methylenebis(1-methyl-1H-imidazol-3-ium) (**a**).* Yield: 79% (based on *N*-Me). Anal. Calc. for $C_9H_{14}Br_2N_4$: C, 31.97; H, 4.17; N, 16.57. Found: C, 32.24; H, 4.26; N: 16.88. IR spectrum (KBr pellet, ν/cm^{-1}): 3458, 3049, 1788, 1641, 1548, 1460, 1331, 1172, 866. LCMS (m/z): 178, 180 M, (M + 2). ^{1}H NMR (400 MHz, δ ppm) (DMSO-d_6): 9.57 (s, 2H, Ar−H), 8.10 (s, 2H, Ar−H), 7.81 (s, 2H, Ar−H), 6.77 (s, 2H, aliphatic-H), 3.89 (s, 6H, *N*-Me).

*3,3′-(Ethane-1,2-diyl)bis(1-methyl-1H-imidazol-3-ium) (**b**).* Yield: 73% (based on *N*-Me). Anal. Calc. for $C_{10}H_{16}Br_2N_4$: C, 34.11; H, 4.58; N, 15.91. Found: C, 34.38; H, 4.68; N: 16.27. IR spectrum (KBr pellet, ν/cm^{-1}): 3435, 3145, 3079, 2854, 2071, 1638, 1556, 1364, 1019, 827. LCMS (m/z): 192, 194 M, (M + 2). ^{1}H NMR (500 MHz, δ ppm) (DMSO-d_6): 9.22 (s, 2H, Ar−H), 7.80−7.82 (d, 2H, Ar−H), 7.74 (s, 2H, Ar−H), 4.24 (s, 4H, aliphatic), 3.86 (s, 6H, *N*-Me).

*3,3′-(Propane-1,3-diyl)bis(1-methyl-1H-imidazol-3-ium) (**c**).* Yield: 82% (based on *N*-Me). Anal. Calc. for $C_{11}H_{18}Br_2N_4$: C, 36.08; H, 4.95; N, 15.30. Found: C, 36.43; H, 4.84; N: 15.79. IR spectrum (KBr pellet, ν/cm^{-1}): 3427, 3148, 3092, 2864, 2069, 1574, 1460, 1340, 1093, 1022, 841. LCMS (m/z): 206, 208 M, (M + 2). ^{1}H NMR (500 MHz, δ ppm) (DMSO-d_6): 9.32 (s, 2H, Ar−H), 7.86 (s, 2H, Ar−H), 7.77 (s, 2H, Ar−H), 4.27 (s, 2H, aliphatic-H), 3.87 (s, 6H, *N*-Me).

dx.doi.org/10.1021/cg3004917 | Cryst. Growth Des. XXXX, XXX, XXX−XXX

*3,3′-(Butane-1,4-diyl)bis(1-methyl-1H-imidazol-3-ium) (**d**).* Yield: 71% (based on *N*-Me). Anal. Calc. for $C_{12}H_{20}Br_2N_4$: C, 37.91; H, 5.30; N, 14.73. Found: C, 37.58; H, 5.36; N: 15.11. IR spectrum (KBr pellet, ν/cm^{-1}): 3430, 3150, 3073, 2958, 2854, 2235, 2054, 1627, 1578, 1326, 1167, 865. LCMS (*m*/*z*): 220, 222 M, (M + 2). ^{1}H NMR (500 MHz, δ ppm) (DMSO-d_6): 9.19 (s, 2H, Ar−H), 7.79 (s, 2H, Ar−H), 7.73 (s, 2H, Ar−H), 4.22 (s, 4H, aliphatic), 3.86 (s, 6H, *N*-Me), 1.78 (s, 4H, aliphatic-H).

*3,3′-(Pentane-1,5-diyl)bis(1-methyl-1H-imidazol-3-ium) (**e**).* Yield: 76% (based on *N*-Me). Anal. Calc. for $C_{13}H_{22}Br_2N_4$: C, 39.61; H, 5.62; N, 14.21. Found: C, 39.89; H, 5.50; N: 14.59. IR spectrum (KBr pellet, ν/cm^{-1}): 3424, 3150, 3095, 3947, 2865, 2476, 1632, 1457, 1167, 838. LCMS (*m*/*z*): 234, 236 M, (M + 2). ^{1}H NMR (500 MHz, δ ppm)) (DMSO-d_6): 9.14 (s, 2H, Ar−H), 7.77 (m, 4H, Ar−H), 4.17 (s, 4H, aliphatic-H), 3.84 (s, 6H, *N*-Me), 1.82 (m, 4H, aliphatic-H), 1.22 (m, 2H, aliphatic-H).

*3,3′-(Hexane-1,6-diyl)bis(1-methyl-1H-imidazol-3-ium) (**f**).* Yield: 81% (based on *N*-Me). Anal. Calc. for $C_{14}H_{24}Br_2N_4$: C, 41.19; H, 5.92; N, 13.72. Found: C, 40.94; H, 6.01; N: 14.26. IR spectrum (KBr pellet, ν/cm^{-1}): 3435, 3148, 3078, 2934, 2085, 1616, 1460, 1338, 1167, 856, 785. LCMS (*m*/*z*): 248, 250 M, (M + 2). ^{1}H NMR (400 MHz, δ ppm) (DMSO-d_6): 9.21 (s, 2H, Ar−H), 7.81 (s, 2H, Ar−H), 7.73 (s, 2H, Ar−H), 4.17 (t, 4H, aliphatic-H), 3.86 (s, 6H, *N*-Me), 1.78 (m, 4H, aliphatic-H), 1.27 (m, 4H, aliphatic-H).

*General Synthetic Procedure for Ion-Pair Compounds **1a**−**1f** (see also Scheme 1).* To a 10 mL MeOH solution of Na_2mnt[20] (2.0 mmol), 5 mL MeOH solution of $CuCl_2{\cdot}2H_2O$ (1.0 mmol) was added, stirred for 30 min at room temperature, and filtered. To this solution, a 15 mL MeOH solution containing $[C_8H_{12}(CH_2)_nN_4]$ (n = 1−6, 1.0 mmol) was added, stirred at room temperature for 2 h, and it was filtered off. The crude (black colored precipitate) product was crystallized from CH_3CN/ether by the diffusion method to give dark-brown crystals for compounds **1a**−**1f**. Single crystals from each compound, suitable for X-ray diffraction study, was selected and characterized structurally. The elemental analyses and routine spectral data for **1a**−**1f** are described below.

*$[C_9H_{14}N_4][Cu(mnt)_2]$ (**1a**).* Yield: 62% (based on copper). Anal. Calc. for $C_{17}H_{14}N_8S_4Cu$: C, 39.10; H, 2.70; N, 21.46. Found: C, 39.38; H, 2.68; N: 21.87. IR spectrum (KBr pellet, ν/cm^{-1}): 3101, 3073, 2263, 2197, 1578, 1545, 1452, 1161, 1117, 793. LCMS (*m*/*z*): 179 (M + H)$^+$. ^{1}H NMR (400 MHz, δ ppm) (DMSO-d_6): 9.34 (s, 2H, Ar−H), 7.94 (s, 2H, Ar−H), 7.80 (s, 2H, Ar−H), 6.62 (s, 2H, aliphatic-H), 3.91 (s, 6H, *N*-Me).

*$[C_{10}H_{16}N_4][Cu(mnt)_2]$ (**1b**).* Yield: 58% (based on Cu). Anal. Calc. for $C_{18}H_{16}N_8S_4Cu$: C, 40.32; H, 3.00; N, 20.89. Found: C, 39.98; H, 3.08; N, 20.45. IR spectrum (KBr, ν/cm^{-1}): 3090, 2262, 2191, 1552, 1460, 1147, 1103, 837, 748. LCMS (*m*/*z*): 193 (M + H)$^+$. ^{1}H NMR (400 MHz, δ ppm) (DMSO-d_6): 9.00 (s, 2H, Ar−H), 7.72 (s, 2H, Ar−H), 7.58 (s, 2H, Ar−H), 4.67 (s, 4H, aliphatic-H), 3.86 (s, 6H, *N*-Me).

*$[C_{11}H_{18}N_4][Cu(mnt)_2]$ (**1c**).* Yield: 60% (based on Cu). Anal. Calc. for $C_{19}H_{18}N_8S_4Cu$: C, 41.18; H, 3.29; N, 20.36. Found: C, 41.56; H, 3.23; N, 20.69. IR spectrum (KBr, ν/cm^{-1}): 3144, 3105, 2359, 2193, 1620, 1572, 1464, 1147, 1049, 862, 760. LCMS (*m*/*z*): 207 (M + H)$^+$. ^{1}H NMR (400 MHz, δ ppm) (DMSO-d_6): 9.11 (s, 2H, Ar−H), 7.75 (s, 4H, Ar−H), 4.23 (s, 4H, aliphatic-H), 3.88 (s, 6H, *N*-Me), 2.40 (s, 2H, aliphatic-H).

*$[C_{12}H_{20}N_4][Cu(mnt)_2]$ (**1d**).* Yield: 57% (based on Cu). Anal. Calc. for $C_{20}H_{20}N_8S_4Cu$: C, 42.57; H, 3.57; N, 19.85. Found: C, 42.89; H, 3.51; N, 19.47. IR spectrum (KBr, ν/cm^{-1}): 3146, 3088, 2197, 1595, 1562, 1464, 1149, 839, 744. LCMS (*m*/*z*): 221 (M + H)$^+$. ^{1}H NMR (400 MHz, δ ppm) (DMSO-d_6): 9.10 (s, 2H, Ar−H), 7.72−7.74 (m, 4H, Ar−H), 4.21 (s, 4H, aliphatic), 3.86 (s, 6H, *N*-Me), 1.79 (s, 4H, aliphatic-H).

*$[C_{13}H_{22}N_4][Cu(mnt)_2]$ (**1e**).* Yield: 61% (based on Cu). Anal. Calc. for $C_{21}H_{22}N_8S_4Cu$: C, 43.62; H, 3.83; N, 19.37. Found: C, 43.30; H, 3.88; N, 18.91. IR spectrum (KBr, cm^{-1}): 3144, 2932, 2355, 2262, 2193, 1556, 1454, 1147, 831, 748. LCMS (*m*/*z*): 235 (M + H)$^+$. ^{1}H NMR (400 MHz, δ ppm) (DMSO-d_6): 9.11 (s, 2H, Ar−H), 7.24 (d, 4H, Ar−H), 4.18 (s, 4H, aliphatic-H), 3.87 (s, 6H, *N*-Me), 1.86 (s, 4H, aliphatic-H), 1.26 (s, 2H, aliphatic-H).

*$[C_{14}H_{24}N_4][Cu(mnt)_2]$ (**1f**).* Yield: 59% (based on Cu). Anal. Calc. for $C_{22}H_{24}N_8S_4Cu$: C, 44.61; H, 4.08; N, 18.91. Found: C, 44.89; H, 4.12; N, 18.59. IR spectrum (KBr pellet, ν/cm^{-1}): 3092, 2361, 2195, 1572, 1462, 1168, 1147, 862, 761. LCMS (*m*/*z*): 249 (M + H)$^+$. ^{1}H NMR (400 MHz, δ ppm) (DMSO-d_6): 9.11 (s, 2H, Ar−H), 7.73 (d, 4H, Ar−H), 4.16 (s, 4H, aliphatic-H), 3.86 (s, 6H, *N*-Me), 1.86 (s, 4H, aliphatic-H), 1.30 (s, 4H, aliphatic-H).

X-ray Diffraction. Data were measured at room temperature for compounds **1a**−**1f** on a Bruker SMART APEX CCD, area detector system [λ (Mo Kα) = 0.7103 Å], graphite monochromator, 2400 frames were recorded with an ω scan width of 0.3°, each for 10 s, crystal-detector distance 60 mm, collimator 0.5 mm.[21] Data reduction was performed with the SAINTPLUS software,[21a] absorption correction using an empirical method SADABS,[21b] structure solution using SHELXS-97 program,[21c] and refined using SHELXL-97 program.[21d] Hydrogen atoms on the aromatic rings were introduced on calculated positions and included in the refinement riding on their respective parent atoms.

RESULTS AND DISCUSSION

Synthesis. We have succeeded in preparing a new series of ion pair compounds with a range of imidazolium cations of varied alkyl chain length (n = 1−6) leading to compounds **1a**−**1f** (see Scheme 1). Compounds **1a**−**1f** are characterized by routine elemental analyses, IR, NMR, UV−visible-NIR spectroscopic techniques, cyclic voltammetry and unambiguously characterized by single crystal X-ray structure determinations. Geometry around the metal ion in complexes **1a**−**1e** is distorted square planar, whereas the geometry of the metal ion in complex **1f** is perfectly square planar. Distortion of these complexes (**1a**−**1e**) can be explained on the basis of the angle between MSS and SCCS planes,[1f] angle c_1−Cu−c_2 (c_1, c_2 are the midpoints between two sulfur atoms from two chelate rings in the anion $[Cu(mnt)_2]^{2-}$), and the angle between two SMS planes (S1CuS2 and S3CuS4) as shown in Scheme 2.

Scheme 2. (a) The Bending Angle (η) in Bent Ligand, (b) the c_1−M−c_2 Angle

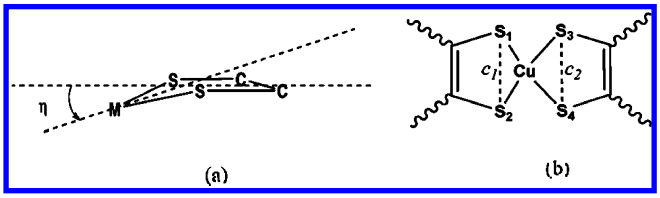

Description of Crystal Structure. *Compound $[C_9H_{14}N_4][Cu(mnt)_2]$ (**1a**).* Crystals of this compound, suitable for X-ray analysis, have been grown from CH_3CN/ether by the diffusion method. Compound **1a** crystallizes in the triclinic system with $P\bar{1}$ space group. The asymmetric unit contains a full molecule; an ORTEP diagram with labeled atoms has been shown in Figure 1a. The basic crystallographic data are presented in Table 1. Here, the overall charge of this Cu(II) complex anion $[Cu(mnt)_2]^{2-}$ as expected is −2, and this anionic charge is compensated by one $[C_9H_{14}N_4]^{2+}$ cation as observed in the crystal structure. In $[Cu(mnt)_2]^{2-}$ anion, the bond lengths of Cu−S are in the range of 2.254(1)−2.269(1) Å, and the bond angles in a chelate ring of SCuS are 92.01°(2) and 92.32°(2). The dihedral angle (λ), which can be defined by the angle between two five-membered rings, that is, S1−Cu−S2 and S3−Cu−S4, is 38.13°, indicates that the copper center in this complex **1a** is deviated from the square-planar coordination geometry. The c_1−Cu−c_2 angle is 176.89°; c_1 and c_2 are the

dx.doi.org/10.1021/cg3004917 | Cryst. Growth Des. XXXX, XXX, XXX−XXX

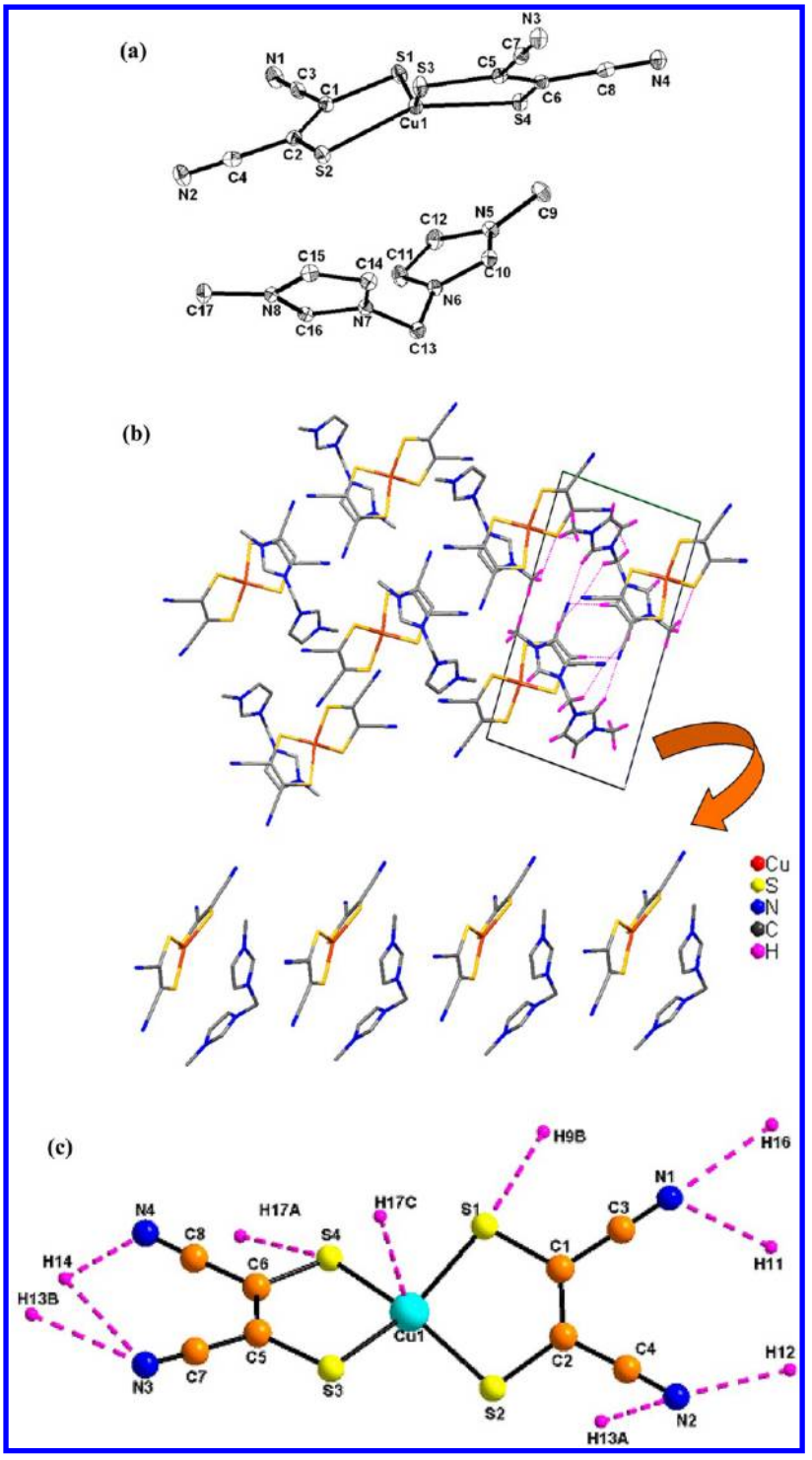

Figure 1. (a) Thermal ellipsoidal diagram of the complex **1a** (with 40% probability), (b) packing diagram of complex **1a**, and (c) hydrogen bonding interactions around the anion $[Cu(mnt)_2]^{2-}$. (Hydrogen bonding interactions are present in the unit cell; remaining are for omitted for clarity.)

midpoints of the two sulfur atoms in the five-membered chelate rings (usually for a perfect square planar complex, the c_1-M-c_2 is 180°). The bending angle (η) between the S3CuS4 and S3C5C6S4 plane is 4.21°, and in the other chelate ring the angle between the S1CuS2 and S1C1C2S2 plane is 0.50°. This indicates that one chelate ring is comparatively more planar than the other chelate ring in the complex anion $[Cu(mnt)_2]^{2-}$. In the solid state, the $[Cu(mnt)_2]^{2-}$ anions (A) and $[C_9H_{14}N_4]^{2+}$ cations (C) are alternately stacked along the crystallographic *c*-axis with a repeating order of ACACAC,[22] and form one-dimensional columns through the $\pi\cdots\pi$ interactions (centroid−centroid) with a range of 3.841−3.966 Å separation between the imidazole moiety from cation and the chelate ring from the anion, which has been shown in Figure 1b. In this complex **1a**, the d(H···A) distance of the C−H···Cu hydrogen bond is 3.14 Å (which is more than the reported value 3.01 Å);[23] the d(D···A) separation of C−H···Cu

dx.doi.org/10.1021/cg3004917 | *Cryst. Growth Des.* XXXX, XXX, XXX−XXX

Table 1. Crystal Data and Structural Refinement Parameters for Compounds 1a−1f

	1a	1b	1c
empirical formula	$C_{17}H_{14}N_8S_4Cu$	$C_{18}H_{16}N_8S_4Cu$	$C_{19}H_{18}N_8S_4Cu$
formula weight	522.14	536.17	550.19
T(K)/λ(Å)	298(2), 0.71073	298(2), 0.71073	298(2), 0.71073
crystal system	triclinic	monoclinic	monoclinic
space group	$P\bar{1}$	$C2/c$	$P2(1)/c$
a (Å)	7.683(7)	18.232(13)	12.2099(15)
b (Å)	9.239(8)	7.228(5)	7.5015(9)
c (Å)	15.405(14)	18.838(14)	26.639(3)
α (°)	90.170(10)	90.00	90.000
β (°)	91.718(10)	111.267(11)	96.688(2)
γ (°)	106.935(10)	90.00	90.000
volume (Å^3)	1046.29(16)	2313(3)	2423.3(5)
Z, ρ_{calcd} (g cm^{-3})	2, 1.637	4, 1.539	4, 1.508
μ (mm^{-1}), F(000)	1.466/530	1.328/1092	1.270/1124
goodness-of-fit on F^2	1.049	1.088	1.050
R_1/wR_2 [$I > 2\sigma(I)$]	0.0262/0.0680	0.0367/0.0855	0.0741/0.1173
R_1/wR_2 (all data)	0.0278/0.0690	0.0400/0.0874	0.1311/0.1361
largest diff peak/hole (e Å^{-3})	0.429/−0.291	0.479/−0.176	0.378/−0.377
	1d	**1e**	**1f**
empirical formula	$C_{20}H_{20}N_8S_4Cu$	$C_{21}H_{22}N_8S_4Cu$	$C_{22}H_{24}N_8S_4Cu$
formula weight	564.27	578.25	592.32
T(K)/λ (Å)	298(2), 0.71073	298(2), 0.71073	298(2), 0.71073
crystal system	monoclinic	triclinic	triclinic
space group	$P2(1)/c$	$P\bar{1}$	$P\bar{1}$
a (Å)	18.1795(12)	8.9511(5)	7.1078(10)
b (Å)	7.6567(5)	11.5301(6)	7.4995(11)
c (Å)	24.6776(12)	12.8835(7)	13.2473(19)
α (°)	90.00	104.497(10)	94.209(2)
β (°)	131.270(3)	95.597(10)	97.374(2)
γ (°)	90.00	98.225(10)	107.625(2)
volume (Å^3)	2480.6(3)	1261.69(12)	662.71(16)
Z, ρ_{calcd} (g cm^{-3})	4, 1.511	2, 1.522	1, 1.484
μ (mm^{-1}), F(000)	1.243/1156	1.224/594	1.167/305
goodness-of-fit on F^2	1.058	1.059	1.051
R_1/wR_2 [$I > 2\sigma(I)$]	0.0398/0.0912	0.0244/0.0620	0.0410/0.1017
R_1/wR_2 (all data)	0.0472/0.0950	0.0252/0.0625	0.0458/0.1048
largest diff peak/hole (e Å^{-3})	0.311/−0.291	0.272/-0.281	0.387/ −0.290

hydrogen bond is 3.943 Å, and the C−H···Cu angle (θ) is 140.7° (see Table 2).

In compound **1a**, there is only one cation which is situated toward the anion through the metal−hydrogen bond (C−H···Cu) with a distance of 3.14 Å, and within the same distance and along that axis no other cation is available on other side of the anion. This implies that there is no center of symmetry along the metal−hydrogen bond through the anion. Around the anion $[Cu(mnt)_2]^{2-}$, there are seven C−H···N and two C−H···S unbalanced interactions, present within the range of 2.34−2.70 Å, and 2.89−2.95 Å, respectively which has been shown in Figure 1c. In its crystal packing, each anion is surrounded by five cations with unbalanced C−H···S, C−H···N supramolecular interactions. On the basis of this data, there is a lack of center of symmetry (Ci) along the Cu···H hydrogen bond and unbalanced interactions around the anion. As a result, the geometry of metal is deviated from square planar coordination. The closest Cu···Cu and Cu···S interactions are 7.688(1) Å and 6.217(3) Å, respectively.

*Compound $[C_{10}H_{16}N_4][Cu(mnt)_2]$ (**1b**).* Suitable sized single crystals of compound **1b** were obtained from the CH_3CN/ether diffusion method. Compound **1b** crystallizes in the monoclinic system with $C2/c$ space group. In its crystal structure, the asymmetric unit contains half of the molecule indicated with labeled atoms. The relevant ORTEP diagram is shown in Figure 2a. The bond lengths of Cu−S are in the range of 2.252(8)−2.265(17) Å and the S−Cu−S angle is 91.63(3)°; this angle is relatively smaller than the corresponding angle in complex **1a.** The dihedral angle (λ) between two SMS planes in $[Cu(mnt)_2]^{2-}$ anion is 32.0°, which is smaller than the corresponding angle in complex **1a**. Thus complex anion $[Cu(mnt)_2]^{2-}$ in **1b** is also not planar. The c_1−Cu−c_2 angle in $[Cu(mnt)_2]^{2-}$ anion of **1b** is 176.66°, indicating that there is a deviation from square-planar geometry at the copper center. The bending angle (η) between S1CuS2 and S1C1C2S2 is 4.28°; it indicates that the chelate ring is near-planar ($\eta < 6°$ indicates highly planar nature of a dithiolene-ligand chelate).[1f] The supramolecular interactions between cation and anion through S···H and N···H hydrogen bonds lead to the formation of a 2-D network. In this network, the cations and anions are arranged in a slippage fashion;[3a,5a] as a consequence there is no significant $\pi\cdots\pi$ interactions between cation and anion (Figure 2b). This slippage fashion interactions in complex **1b**, between cation and anion through S···H and N···H hydrogen bonds (2.84−2.87 Å and 2.52−2.75 Å respectively) leads to shorter intermolecular contacts, 3.614(4) Å for C(7)···S(1) and 3.340(5) Å for C(6)···N(1); the rest of the hydrogen bonding interactions are described in a table in section-13 of Supporting Information. The C−H···Cu hydrogen bond in compound **1b** is characterized by H···Cu separation (d) 3.05 Å, C−H···Cu distance (D) 3.920 Å and the C−H···Cu (θ) angle 150.9°,

Table 2. Supramolecular Interaction between Hydrogen from the Cation to Metal from the Anion (Bond Lengths in Å and Bond Angles in °)

compound	D−H···A	d(H···A)	d(D···A)	∠(DHA)	symmetry code
1a	C(17)−H(17C)···Cu1	3.14	3.943(2)	140.7	$x, y-1, z$
1b	C(5)−H(5A)···Cu1	3.05	3.920(4)	150.9	$x+1, y, z$
1c	C(12)−H(12A)···Cu1	2.98	3.865(7)	151.6	$x, y-1, z$
	C(12)−H(12B)···Cu1	3.06	3.877(7)	142.8	x, y, z
1d	C(12)−H(12C)···Cu1	3.07	3.828(3)	137.2	$x, -y+1.5, z+0.5$
	C(20)−H(20C)···Cu1	3.11	3.708(4)	121.8	$x, y+1, z+1$
1e	C(20)−H(20)···Cu1	2.91	3.395(18)	112.6	$1-x, 1-y, 1-z$
1f	C(8)−H(8C)···Cu1	2.72	3.614(4)	156.2	x, y, z

dx.doi.org/10.1021/cg3004917 | Cryst. Growth Des. XXXX, XXX, XXX−XXX

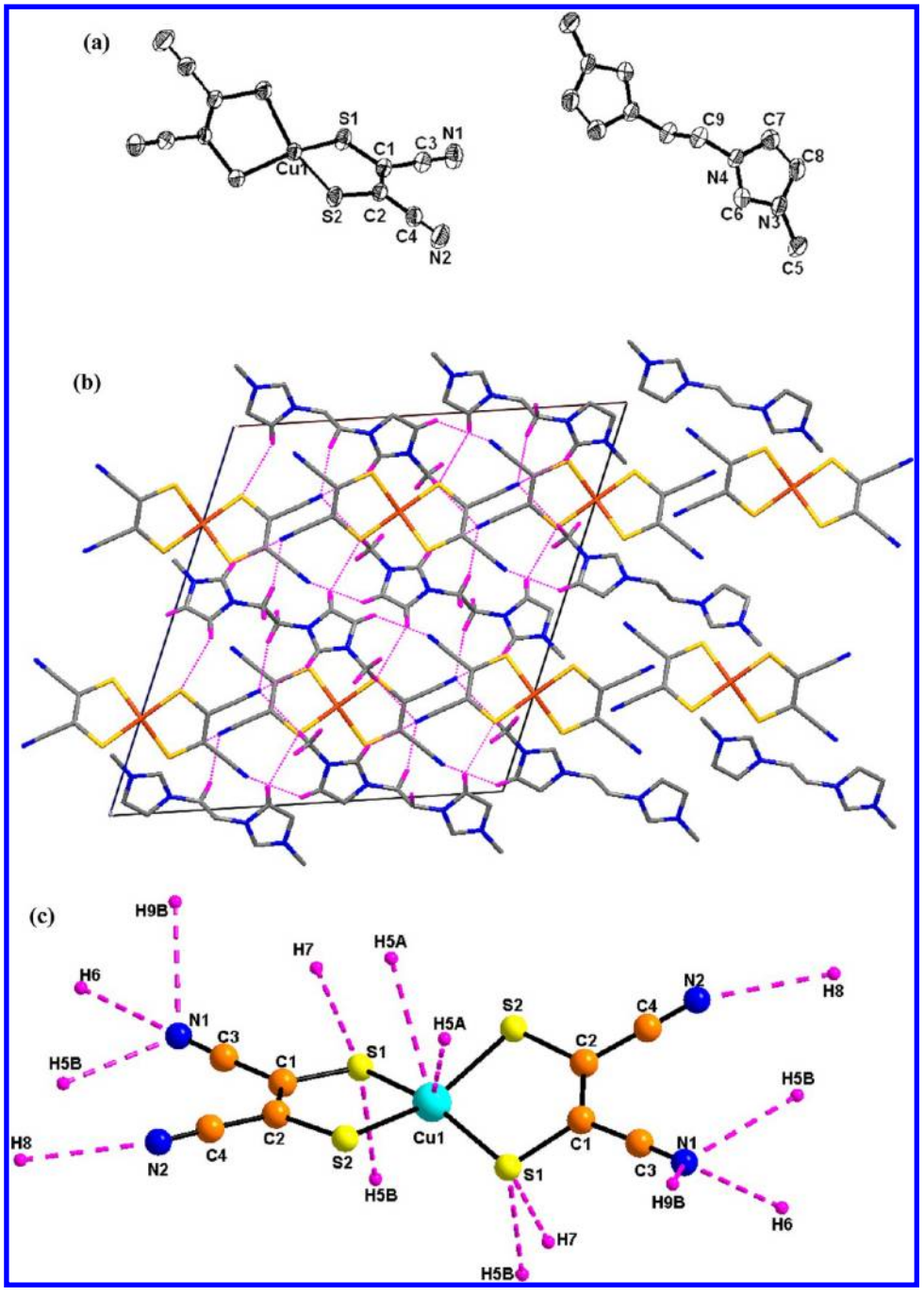

Figure 2. (a) Thermal ellipsoidal diagram of the complex **1b** (with 40% probability), (b) packing diagram of complex **1b**, and (c) hydrogen bonding interactions around the anion $[Cu(mnt)_2]^{2-}$.

which are closed to the relevant literature values.[23] In this compound, there are two cations are present at the same side of the anion with a distance of 3.05 Å through metal−hydrogen interactions, which clearly indicates that there is no center of symmetry (*Ci*) along the metal−hydrogen bond. Around the complex anion, there are balanced S···H and N···H interactions (Figure 2c, each chelate ring is interacted with identical distances), but in the case of Cu···S contacts, these are unbalanced interactions. As described in the section 1 of Supporting Information, the Cu1···S1 separation is 7.18 Å and Cu1···S2 separation is 7.09 Å, which indicates sulfur atoms (S1 and S2) from two chelate rings in the anion interact with copper differently. On the basis of the lack of center or symmetry and unbalanced supramolecular interactions, the structure of the anion in complex **1b**, is deviated to distorted square planar.

*Compounds $[C_{11}H_{18}N_4][Cu(mnt)_2]$ (**1c**) and $[C_{12}H_{20}N_4][Cu(mnt)_2]$ (**1d**).* Dark brown crystals of these two complexes suitable for X-ray structure analysis have been grown from CH_3CN/ether by the diffusion method. Both compounds **1c** and **1d** crystallize in $P2(1)/c$ space group in the monoclinic system. In their crystal structures, the asymmetric unit contains the full molecule as represented with labeled atoms in Figures 3a and 4a, respectively. The Cu−S bond lengths in compounds **1c** and **1d** are in the range of 2.246−2.266 Å and 2.258−2.273 Å, respectively. Notably, there is a short Cu−S bond length

dx.doi.org/10.1021/cg3004917 | *Cryst. Growth Des.* XXXX, XXX, XXX−XXX

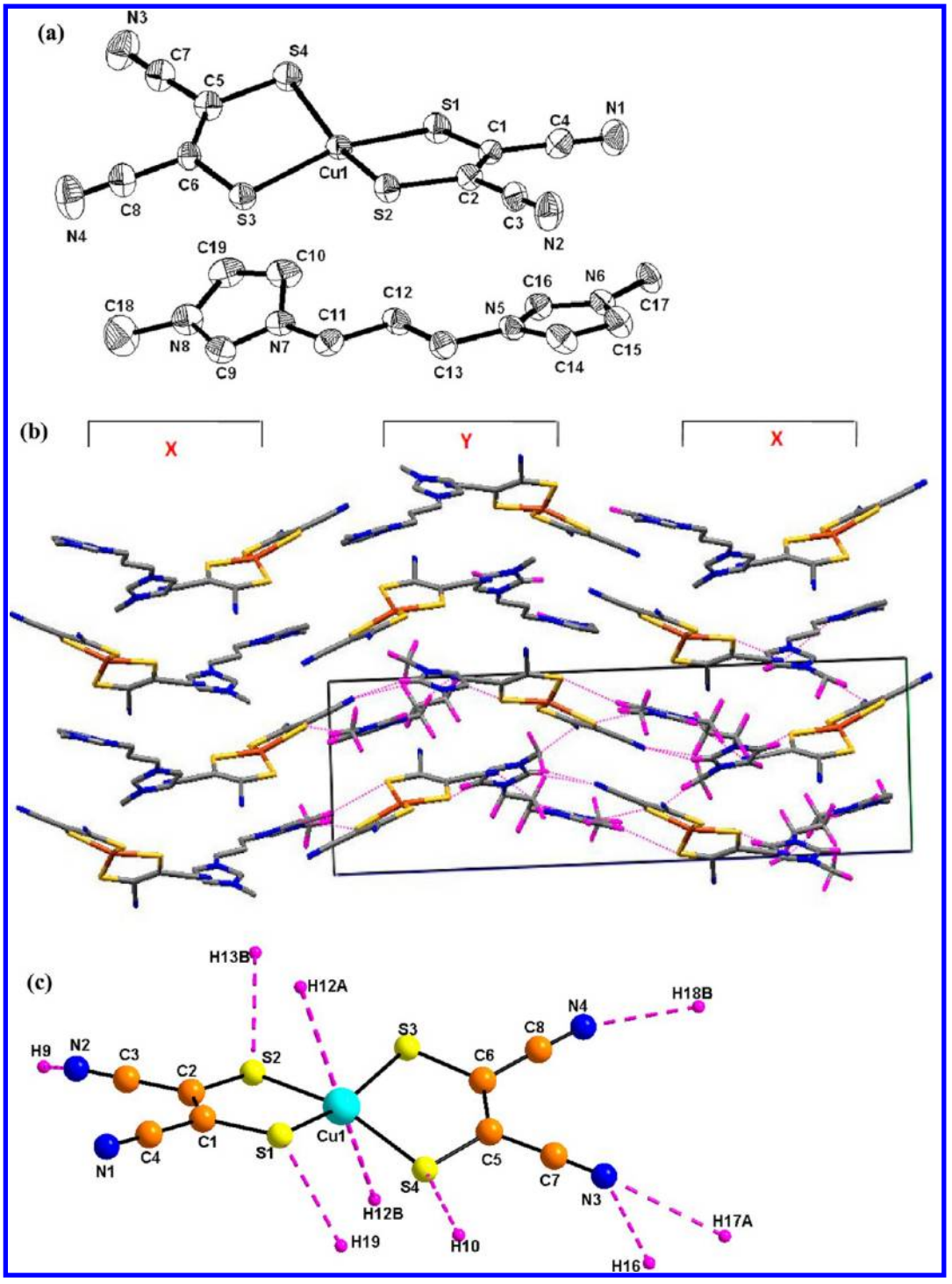

Figure 3. (a) Thermal ellipsoidal diagram of the complex **1c** (with 30% probability), (b) packing diagram of complex **1c**, and (c) hydrogen bonding interactions around the anion $[Cu(mnt)_2]^{2-}$.

(Cu(1)−S(4) = 2.246(18) Å) in compound **1c**, which is shorter than Cu−S bonds in the crystal structures of compounds **1a** and **1b**. On the other hand, the Cu(1)−S(1) bond length of 2.273(1) Å in compound **1d** is longer than Cu−S bonds in the crystal structures of compounds **1a** and **1b**. The S−Cu−S bond angles in the anion $[Cu(mnt)_2]^{2-}$ of compounds **1c** and **1d** are in the range of 91.39(6)−91.81(7)° and 91.37(3)−91.56(3)°, respectively. The deviation angles (λ) with respect to perfect square-planar geometry, which can be measured as the angle between two S−Cu−S planes in two chelate rings present in $[Cu(mnt)_2]^{2-}$ anions of the compounds **1c** and **1d**, are found to be 26.73° and 19.91°, respectively. These angles are relatively smaller as compared to those in the above-discussed compounds **1a** and **1b**. The c_1−Cu−c_2 angles in compounds **1c** and **1d** are 179.22° and 178.48°, respectively. The related bending angles (η) in the anion $[Cu(mnt)_2]^{2-}$ of **1c** and **1d** are 6.45°, 3.28° and 2.49°, 3.59°, respectively. Thus each chelate ring deviates from the planar arrangement. The supramolecular interactions between cation and anion through S···H and N···H contacts lead to 2-D

dx.doi.org/10.1021/cg3004917 | *Cryst. Growth Des.* XXXX, XXX, XXX−XXX

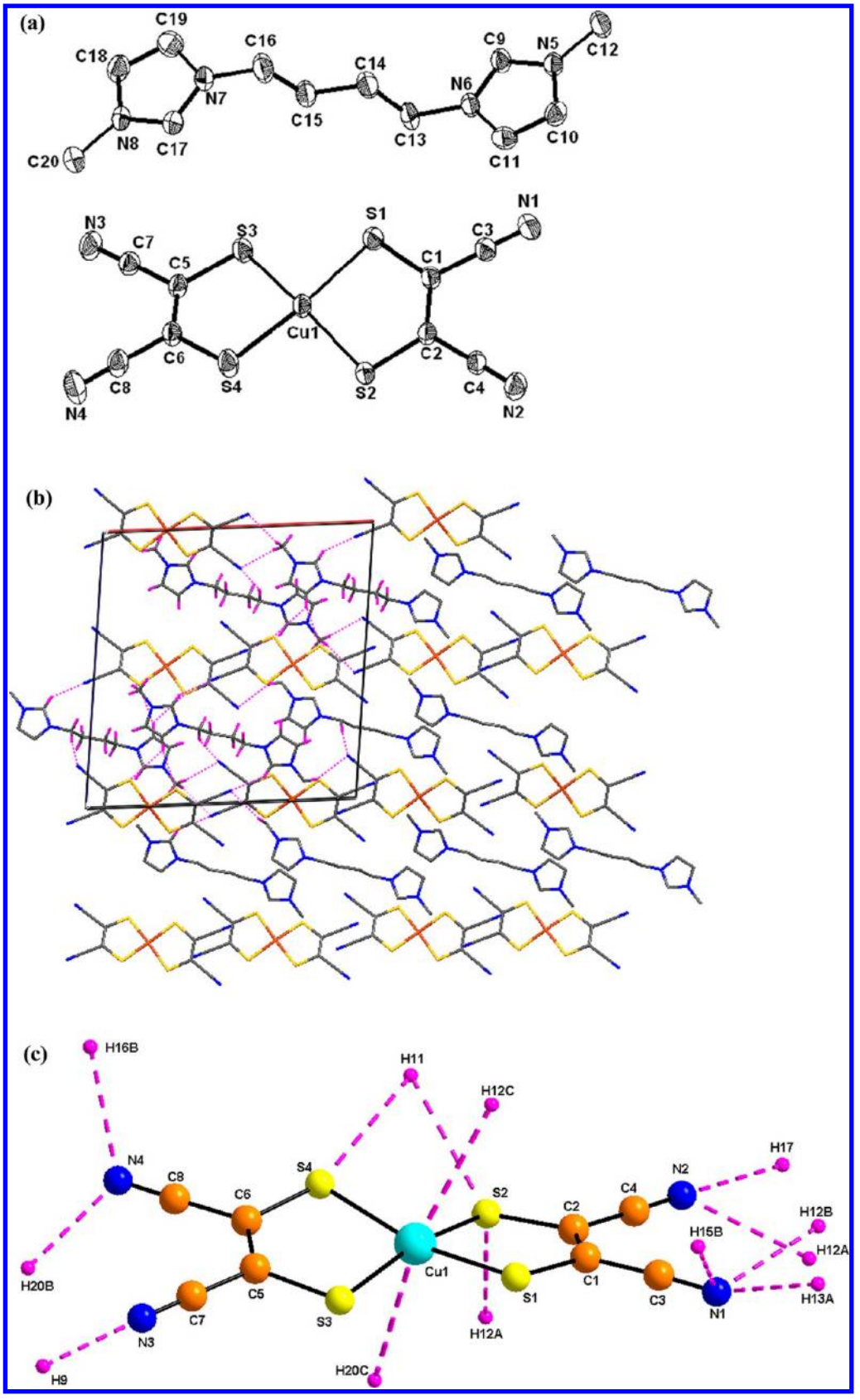

Figure 4. (a) Thermal ellipsoidal diagram of the complex **1d** (with 30% probability), (b) packing diagram of complex **1d**, and (c) hydrogen bonding interactions around the anion $[Cu(mnt)_2]^{2-}$.

network structures (Figures 3b and 4b for compounds **1c** and **1d**, respectively). As shown in Figure 3b for the crystal structure of compound **1c**, there are two different arrangements (named as X and Y) of cations and anions. In both

dx.doi.org/10.1021/cg3004917 | *Cryst. Growth Des.* XXXX, XXX, XXX−XXX

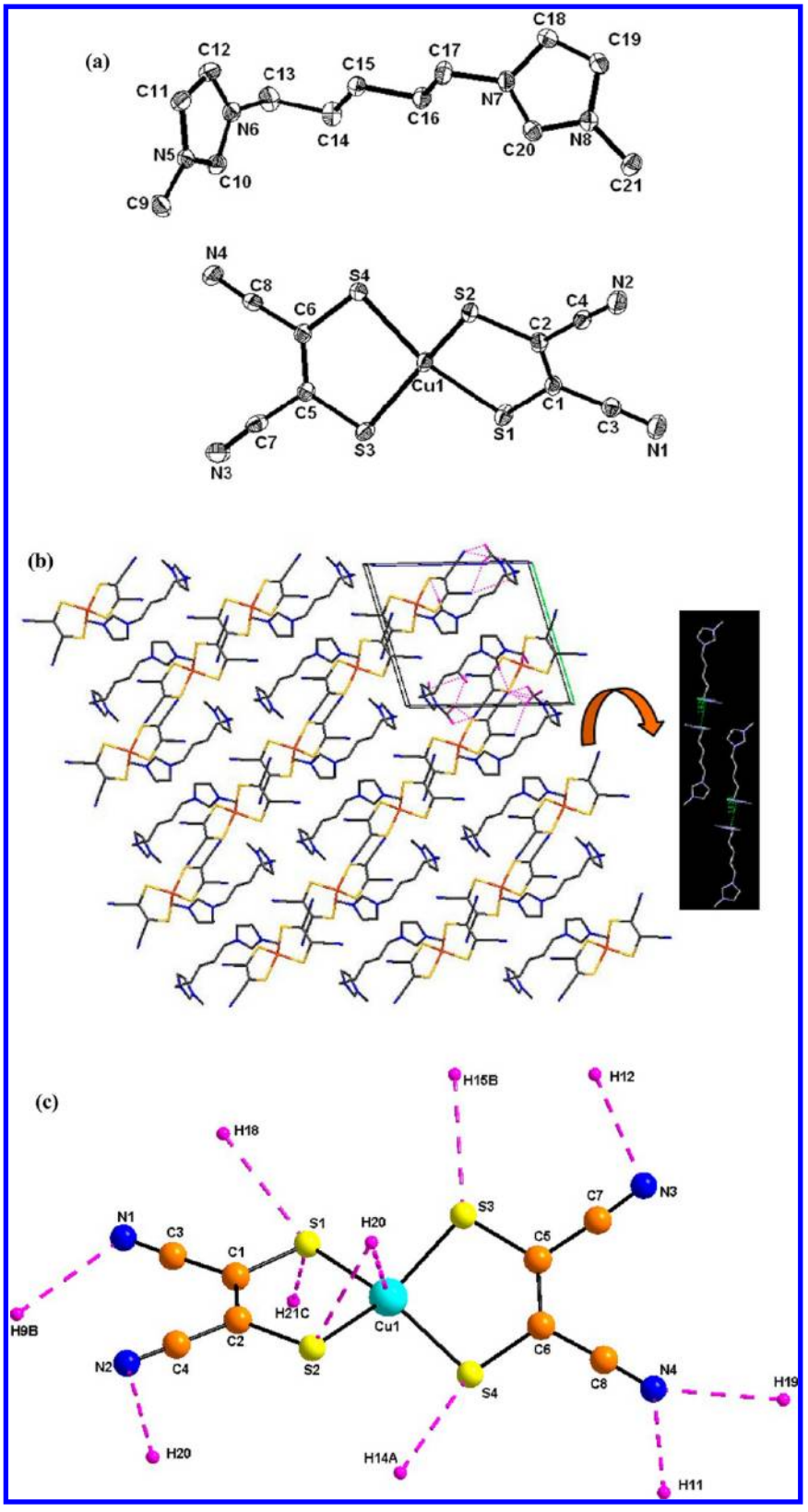

Figure 5. (a) Thermal ellipsoidal diagram of the complex **1e** (with 50% probability), (b) packing diagram of complex **1e**, and (c) hydrogen bonding interactions around the anion $[Cu(mnt)_2]^{2-}$.

arrangements X and Y, there is a stacking of cation−anion (C-A). The C-A in the X column is mirror image to the C-A of the Y column. The packing arrangement of crystal structure of compound **1c** can be described as X Y X Y X Y and so on (Figure 3b). In the crystal structure of **1d**, there is a slippage arrangement of the cations and anions, which is similar to that in the crystal structure of compound **1b** (vide supra), except there is a small change in the alignment of cations compared to

dx.doi.org/10.1021/cg3004917 | *Cryst. Growth Des.* XXXX, XXX, XXX−XXX

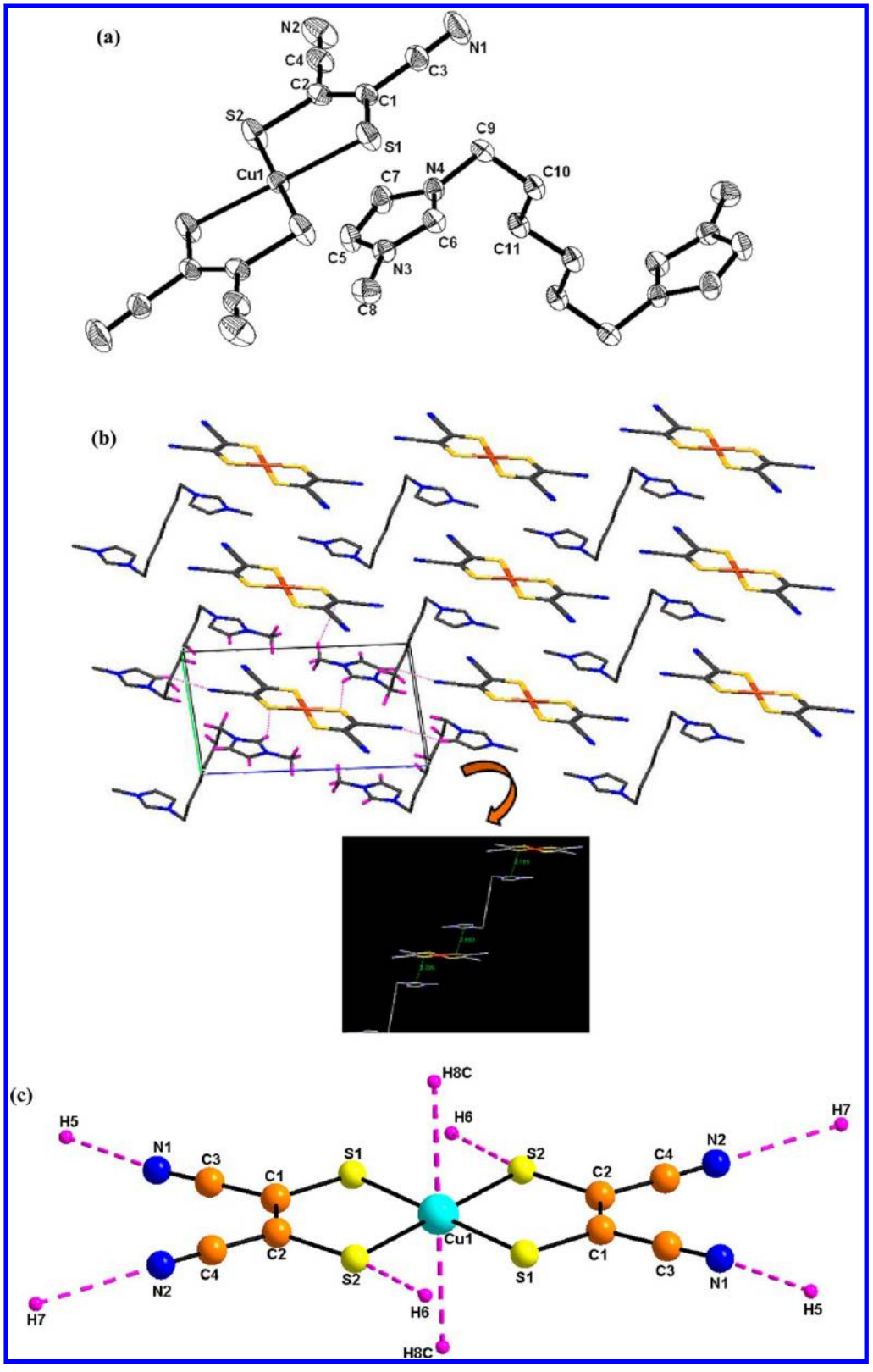

Figure 6. (a) Thermal ellipsoidal diagram of the complex **1f** (with 30% probability), (b) packing diagram of complex **1f**, and (c) hydrogen bonding interactions around the anion $[Cu(mnt)_2]^{2-}$.

that in compound **1b**. The Cu···H separation (d), C−H···Cu distance (D), and C−H···Cu angle (θ) are 2.98 Å, 3.86 Å and 151.6° respectively for compound **1c**, and 3.067 Å (d) 3.828 Å (D) and 137.2° (θ), respectively for compound **1d**. The intermolecular separations of Cu···Cu and Cu···S are 6.774 Å, 5.376 Å and 7.357 Å, 6.975 Å, for the compounds **1c** and **1d**, respectively.

In compound **1c**, two cations are present at top and bottom of the complex anion $[Cu(mnt)_2]^{2-}$ with a different distances (2.98 Å and 3.06 Å) of C−H···Cu interactions. This clearly

dx.doi.org/10.1021/cg3004917 | *Cryst. Growth Des.* XXXX, XXX, XXX−XXX

indicates that there is no center of symmetry along the metal−hydrogen bond interaction. Sulfur atoms (S1, S2, and S4) from the chelate rings interact with two different surrounding cations with symmetry code (#10, #11) operations. From the complex anion $[Cu(mnt)_2]^{2-}$, S1 and S4 interact with a common cation $[C_{11}H_{18}N_4]^{2+}$ through C−H(19)···S1, C−H(10)···S4 hydrogen bonds with distances of 2.93 and 2.98 Å respectively. A seven-membered ring consisting of Cu1S1H19C19C10H10S4 with C−H···S interactions is observed (Section-1 in Supporting Information), and around the anion there are totally seven different S···H and N···H interactions that are present with three surrounding cations, as shown in Figure 3c. In compound **1c**, the structure of the anion is deviated from planarity due to the lack of a center of symmetry (*Ci*) along the interaction of metal−hydrogen bond and unbalanced supramolecular interactions around the anion. In compound **1d**, there are two metal hydrogen bonding interactions of the complex anion with surrounding huge cations $[C_{12}H_{20}N_4]^{2+}$, that are situated at top and bottom of the anion with 3.07 Å and 3.11 Å of distances. Thus, there is no center of symmetry along the metal−hydrogen bond in the complex **1d**. Seven cations interact with the anion through eight C−H···N and three C−H···S supramolecular interactions. A four-membered ring (Cu1S2H11S4) is observed in which two sulfur atoms (S2 and S4) from the two chelate rings are connected to the cation through common hydrogen bonds (C−H(11)···S2, C−H(11)···S4) with distances of 2.95 Å and 3.00 Å respectively as shown in Figure 4c. Because of this interaction, movement of two chelate rings is restricted (S2 and S4 atoms are interacted to the cation with a common hydrogen bond). This indicates that there is no center of symmetry along the metal−hydrogen bond in compound **1d**, and due to unbalanced supramolecular interactions, coordination geometry of metal ion is deviated to the distorted square planar.

Compound $[C_{13}H_{22}N_4][Cu(mnt)_2]$ *(**1e**).* Compound **1e** crystallizes in $P\bar{1}$ space symmetry (triclinic) with half of the molecule present in its asymmetric unit (Figure 5a). The average Cu−S bond length and S−Cu−S bond angle in $[Cu(mnt)_2]^{2-}$ anion are 2.261 Å and 92.19°, respectively. The dihedral angle (λ) in the $[Cu(mnt)_2]^{2-}$ anion is 37.06°, which is larger than those in compounds **1b**−**1d**, but this angle is comparable to that in compound **1a**. In compound **1e**, the $[Cu(mnt)_2]^{2-}$ anion is a nonplanar structure and all the nitrogen atoms are deviated from mean plane of {S1S2S3S4} (N1: 0.878 Å, N2: 0.408 Å, N3: 0.990 Å and N4: 0.565 Å). The bending angle (η) in one chelate ring (Cu1S1C1C2S2) is 4.21°, and in the other chelate ring (Cu1S3C5C6S4) it is 0.56°, which indicates that one of the chelate ring in the $[Cu(mnt)_2]^{2-}$ anion is more deviated from the planarity than the other chelate ring. The bending angles in compound **1e** are similar to those in compound **1a** (η = 4.21°, 0.50°). In the cationic part of its molecular structure, the angle between planes of two imidazole moieties is 67.07°, which is 55.11° in compound **1a**. The supramolecular S···H and N···H interactions lead the formation of a 2-D network, in which cations and anions are arranged in slippage fashion as shown in the case of compound **1b** (vide supra). There are $\pi\cdots\pi$ (Cg1−Cg2) stacking interactions between imidazole moieties (Cg1 = {C9C10C11N5N6}, and Cg2 is symmetry related equivalent of Cg1) from individual cations, in which each cation is positioned in between two $[Cu(mnt)_2]^{2-}$ anion moieties as shown in Figure 5b. Intermolecular Cu···Cu and Cu···S separations are 6.940 Å and 6.025 Å, respectively. The d(H···A) distance of C−H···Cu hydrogen bond in compound **1e** is 2.91 Å, with an angle (θ) of 112.6°. The cationic moiety laying above the plane of the $[Cu(mnt)_2]^{2-}$ anion interacts with the complex anion $[Cu(mnt)_2]^{2-}$ via C−H···Cu distance of 2.91 Å. The non-appearance of any cationic moiety just below the plane of the complex anion $[Cu(mnt)_2]^{2-}$ (i.e., other side of the plane of the complex anion) indicates the lack of a center of symmetry along the metal hydrogen interaction. In the crystal structure of compound **1e**, each anion interacts with five cationic units through C−H···S and C−H···N type of hydrogen bonding interactions as shown in Figure 5c. The unbalanced supramolecular interactions around complex anion $[Cu(mnt)_2]^{2-}$ results in the distorted square planar geometry of the complex anion $[Cu(mnt)_2]^{2-}$.

Compound $[C_{14}H_{24}N_4][Cu(mnt)_2]$ *(**1f**).* Compound **1f** crystallizes in triclinic space group $P\bar{1}$. Figure 6a shows the asymmetric unit with half of the molecule. The angle between two SMS planes is zero, that is, the c_1−Cu−c_2 angle is 180°, which indicates that the dihedral angle between two SCuS planes is 0°; therefore in compound **1f**, the complex anion $[Cu(mnt)_2]^{2-}$ is perfectly square planar. This is in contrast to the situation in compounds **1a**−**1e**. In **1f**, the bending angles (η) between two chelate rings in the $[Cu(mnt)_2]^{2-}$ anion is 0° which supports the nondeviation from planarity in the complex anion. The molecular structure shows $\pi\cdots\pi$ interactions between Cg1 and Cg2 chelated rings (Cg1 = Cu1S1S2C1C2 from coordination complex anion moiety and Cg2 = N3C5C6C7N4 from imidazole cation moiety) with a distance of 3.785 Å (Figure 6b). The supramolecular interactions (S···H, N···H, and Cu···S) around each chelate ring in the complex anion are identical (see section 1 in Supporting Information) resulting in balanced interactions around the complex anion. The d(H···A) separation and the d(D···A) distance of C−H···Cu hydrogen bond and C−H···Cu angle (θ) are 2.72 Å, 3.614 Å, and 156.2° respectively. These supramolecular interactions lead to the formation of a 1-D chain. The geometrical parameters for the above-mentioned metal hydrogen supramolecular interactions for all the compounds **1a**−**1f** are described in Table 2.

In **1f**, around the complex anion there are two cations are present: one cation is situated at the top of the complex anion and the other cation at the bottom of the complex anion with a same distance of 2.72 Å for C−H···Cu interactions. This clearly indicates there is a center of symmetry (*Ci*) along the interaction of metal hydrogen bond through the anion. In this compound, six cations interact to the anion through equivalent distances of two C−H···S and four C−H···N hydrogen bonds as shown in Figure 6c. In addition to these, we observe equivalent distances out of metal and sulfur interactions. All these indicate that there are balanced equivalent interactions, present around the complex anion. Hence, the geometry around the central metal ion of the complex anion is perfectly square planar. Following Scheme 2, the MSC and SCC angles in complex anion $[Cu(mnt)_2]^{2-}$ of compound **1f** are 102.0° and 122.71 respectively. The same parameters in the complex anion $[Cu(mnt)_2]^{2-}$ of compound **1a** are 100.71° and 123.15°, respectively. As shown in Figure 7, the larger MSC angles are offset by smaller SCC angles.[1f]

Discussion about the Distortion in Square-Planar Complexes. The deviation from the planarity in the series of above-described square planar complexes can be explained by considering the following factors: lack of center of symmetry (*Ci*) along metal hydrogen bond, unbalanced supramolecular

dx.doi.org/10.1021/cg3004917 | *Cryst. Growth Des.* XXXX, XXX, XXX−XXX

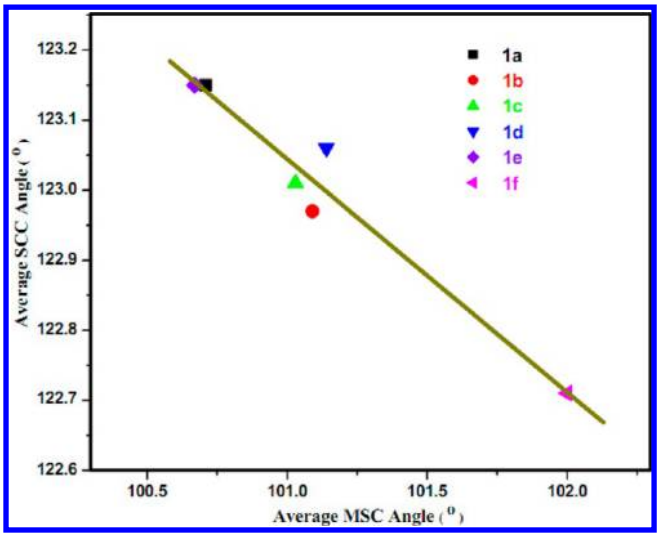

Figure 7. Plot between angles (Å) of MSC and SCC in the anion $[Cu(mnt)_2]^{2-}$ of the complexes **1a−1f**.

interactions and crowdedness around the complex anion $[Cu(mnt)_2]^{2-}$. If a line is drawn through a point in the molecule in one direction and extended to equal distance in the opposite direction meeting another similar group or atom, then the point (generally the central metal ion) is called the center of symmetry (*Ci*). As shown in Scheme 3a, there is a center of symmetry along the interaction of the metal hydrogen bond in which the metal is Cu^{2+} ion of the complex anion $[Cu(mnt)_2]^{2-}$, showing identical hydrogen bonds from both sides of the anion with an identical distance. There are symmetrical or balanced interactions around the anion that are shown in purple color in Scheme 3b. The same Scheme 3b also shows unbalanced supramolecular interactions involving different groups with dissimilar distances as indicated in green color. This leads to a change in spatial orientation of the chelate rings of the anion. Scheme 3c presents the possibility that in the crystals of the above-mentioned compounds (**1a−1f**), the required cations are present closed to the complex anion and interact from top/bottom of molecular plane of the complex anion with a metal hydrogen bond. The geometry around the metal ion of the coordination complex anion $[Cu(mnt)_2]^{2-}$, naturally, depends on the crowdedness or bulkiness of the cations in the relevant ion pair compound. Now we discuss the deviation of the molecular plane of the complex $[Cu(mnt)_2]^{2-}$ in compounds **1a−1f** with respect to the geometry around copper ion based on the above-described factors, namely, center of symmetry, unbalanced/unsymmetrical interactions and crowdedness/bulkiness of the interacting groups.

In compound **1a**, there is one noncovalent metal hydrogen bond (C−H···Cu) with a distance of 3.14 Å; this indicates within this distance, there is a cation $[C_9H_{14}N_4]^{2+}$ hydrogen bonded to $[Cu(mnt)_2]^{2-}$ anion from one side. Moreover, there are unbalanced supramolecular S···H, N···H interactions around the complex anion $[Cu(mnt)_2]^{2-}$ (Figure 1c). The combination of these two factors leads to a considerable amount of distortion around the copper ion with a dihedral angle of 38.13°. In the case of compound **1b**, there are two noncovalent metal hydrogen bonds (C−H···Cu) with a distance of 3.05 Å; however, both cation moieties $[C_{10}H_{16}N_4]^{2+}$ are hydrogen bonded from same side of the $[Cu(mnt)_2]^{2-}$ anion (Figure 2c). Thus the occurrence of a center of symmetry along the metal−hydrogen bond is not possible in this case. Unbalanced supramolecular interactions are relatively lesser than those in compound **1a**. So the dihedral angle (λ) for the complex anion in **1b** is decreased to 32.0° (see Supporting Information). In the case of compound **1c**, two cation moieties $[C_{11}H_{18}N_4]^{2+}$ are attached to the $[Cu(mnt)_2]^{2-}$ anion by C−H···Cu hydrogen bond from opposite sides (e.g., from top and bottom) of the molecular plane (Figure 3c). Similarly two cationic moieties of $[C_{12}H_{20}N_4]^{2+}$ are glued to $[Cu(mnt)_2]^{2-}$ by two C−H···Cu hydrogen bonds from top and bottom of the molecular plane in compound **1d** (Figure 4c). Thus the potential of unbalanced supramolecular interactions is considerably reduced and thereby the deviation of the chelate rings in $[Cu(mnt)_2]^{2-}$ is accordingly reduced. This leads to further decrease in the deviation angle (26.73°) in complex **1c** in comparison to that in **1a** and **1b**. In the case of compound **1d**, two chelate rings of $[Cu(mnt)_2]^{2-}$ anion are linked by a common C−H···S interaction (bifurcated hydrogen bonds), thereby restricting the chelate rings considerably from deviation. Therefore the relevant deviation angle is drastically reduced to 19.91° in compound **1d**. For the compound **1e**, the noncovalent C−H···Cu hydrogen bond separation is 2.91 Å, which is too short a distance for a huge cation $[C_{13}H_{22}N_4]^{2+}$ to interact with the complex anion $[Cu(mnt)_2]^{2-}$; thus it affects the distortion of the chelate rings to a larger extent resulting in the deviation angle of 37.06° (Figure 5c). Finally in compound

Scheme 3. (a) Center of Symmetry along Metal−hydrogen Interaction, (b) Equivalent and Unequivalent Hydrogen Bonding Interactions, (c) Bulkiness around the Anion $[Cu(mnt)_2]^{2-}$

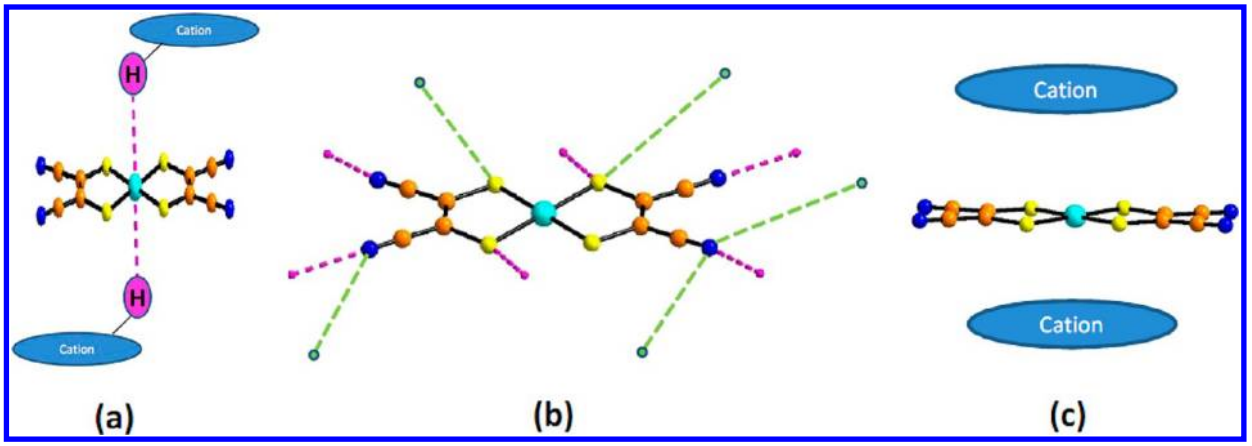

dx.doi.org/10.1021/cg3004917 | *Cryst. Growth Des.* XXXX, XXX, XXX−XXX

1f, two cationic moieties of $[C_{14}H_{24}N_4]^{2+}$ are hydrogen bonded to $[Cu(mnt)_2]^{2-}$ with C−H···Cu hydrogen bond separation of 2.72 Å. Even though this distance is too short for a huge cation, these two cation moieties $[C_{14}H_{24}N_4]^{2+}$ are glued from opposite sides of the molecular plane maintaining same distance of 2.72 Å leading to the center of symmetry along the metal hydrogen bond. In addition, there are balanced C−H···S, C−H···N, and Cu···S supramolecular interactions around the $[Cu(mnt)_2]^{2-}$ anion. The combination of the center of symmetry and balanced supramolecular interactions lead to the perfect square planar arrangement of $[Cu(mnt)_2]^{2-}$ with zero deviation angle.

On the basis of the above discussion, it can be concluded that unbalanced supramolecular S···H, N···H, and Cu···S interactions are observed in compounds **1a**−**1e**. Bulkiness or occupancy nature of cations increase from compound **1a** to compound **1f**. The flexibility of chelate rings of the $[Cu(mnt)_2]^{2-}$ anion is restricted through surrounding supramolecular interactions. Movement of the chelate ring depends on the number of interactions with surrounding cations in ion-pair compounds. In case of compound **1f**, we observe that there is a center of symmetry along the metal−hydrogen bond and there are equivalent or balanced C−H···S, C−H···N, and Cu···S supramolecular interactions around $[Cu(mnt)_2]^{2-}$ resulting in perfect square planar arrangement of $[Cu(mnt)_2]^{2-}$ in compound **1f**. There is an equivalent force along all the sides of anion $[Cu(mnt)_2]^{2-}$, which implies that there is no more distortion from the square planar nature. Diagrammatic representation of the cations which are linked to the anion through the interaction of metal hydrogen bond is shown in section-1 of Supporting Information.

Spectroscopic and Electronic Characterization. *Electronic Absorption Spectra.* Absorption spectra of the title compounds are measured in acetonitrile. For the entire ion-pair compounds **1a**−**1f**, we have observed five absorption bands (see in section-9 in Supporting Information) in the range of 200−1300 nm, in which there are four intense bands due to allowed transitions. Bands at 270, 370 nm are assigned due to the L → M charge transfer transitions of $[Cu(mnt)_2]^{2-}$. Bands at 320 and 470 nm can be attributed as L → L* and M → L charge transfer transition, respectively.[24]

On the basis of the literature,[25] the copper based dithiolene complex $[TBA]_2[Cu(mnt)_2]$ shows an absorption band in the near-IR region at 1205 nm (ε = 70 M^{-1} cm^{-1}). In the present study, copper based ion-pair dithiolene compounds **1a**−**1f** show a moderate absorbance at the near-IR region (1210 nm) with a slight variation of molar extinction coefficient (ε = 76 to 122 M^{-1} cm^{-1}), which has been shown in section 10 of Supporting Information. Absorption spectra, that are characteristic of metal-bis(dithiolene) ion-pair complexes, are generally assigned to $\pi \rightarrow \pi^*$ transition between the highest occupied molecular orbital (HOMO) of the $[Cu(mnt)_2]^{2-}$ anion and the lowest unoccupied molecular orbital (LUMO) of the alkyl chain imidazolium cation. In the solution absorption spectra, there is no shifting of the peak position for the complexes **1a**−**1f**.

In the diffuse reflectance spectra (Figure 8), we observe the band in the near-IR region for all compounds **1a**−**1f**. Usually square-planar copper complexes show a peak at 1150 nm in the near-IR region. But, from Figure 8, we observe that the peak positions for the complexes **1a**−**1f** vary within the range 1121−1268 nm. This indicates that the copper complexes with more deviation angle exhibit a strong bathochromic shift of the near-IR band compared to the copper complexes with less deviation angle. This shift amounts to 147 nm in the case of dithiolato-complexes from **1a** to **1f**. The deviation angle for the complex **1a** is more (λ = 38.13°) than those for the remaining complexes; thus the peak position for **1a** is 1268 nm. For the remaining complexes **1b**−**1d**, the decrease in deviation angle order is **1b** > **1c** > **1d**, and hence the peak position also decreases in a similar manner 1218 > 1163 > 1137 nm, respectively. In the case of complex **1e**, the deviation angle is 37.06°, which is almost identical to that of complex **1a**, so that peak position is shifted accordingly to the longer wavelength 1258 nm region. Finally compound **1f** having a deviation angle of 0° shows the peak position at 1121 nm, which is comparable to that of the square planar complex $[TBA]_2[Cu(mnt)_2]$ showing a peak position at 1120 nm. From these solid state absorption studies, it can be concluded that the energy gap between HOMO of the anion and LUMO of the cation is decreased in the case of complexes with more deviated angles.[5a]

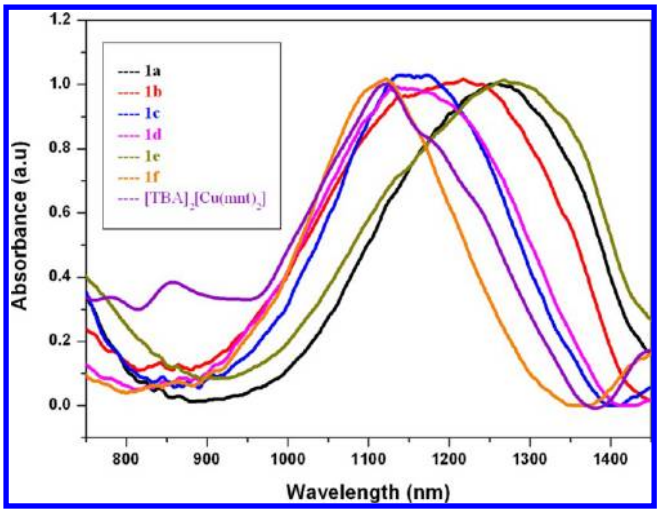

Figure 8. Diffuse reflectance spectra of complexes **1a**−**1f** and $[TBA]_2[Cu(mnt)_2]$.

Electrochemistry. The electrochemical behavior of the complexes **1a**−**1f** in acetonitrile solutions have been studied, each containing 0.10 M $[Bu_4N][ClO_4]$ (TBAP) as a supporting electrolyte at a platinum working electrode. The cyclic voltammograms are shown in section-11 of Supporting Information. A representative cyclic voltammogram (compound **1c**) is shown in Figure 9. The cyclic voltammograms of copper compounds **1a**−**1f** exhibit an oxidative response. The present electrochemical data can be explained on the basis of Scheme 4, proposed by McCleverty, Hoyer, and others.[26] According to this scheme, the first oxidative response for compounds **1a**−**1f** are ascribed due to the couple $[Cu^{III}(mnt)_2]^{1-}/[Cu^{II}(mnt)_2]^{2-}$. Oxidative responses at $E_{1/2}$ = +0.494, +0.461, +0.522, +0.511, +0.510, +0.504 V vs Ag/AgCl are for compounds **1a**−**1f** respectively. We did not attempt to assign the second oxidative responses for these compounds. We undertook the electrochemical studies of title compounds **1a**−**1f** to investigate the influence of alkyl imidazolium cation on the red-ox potential of complex anion $[Cu^{II}(mnt)_2]^{2-}$ by comparing present electrochemical data (compound **1a**−**1f**) with those of $[TBA]_2[Cu(mnt)_2]$. We found that first oxidative responses of compounds **1a**−**1f** (present study) agrees quite well with that reported for the $[TBA]_2[Cu(mnt)_2]$ complex.[25] This suggests that there is not much effect of alkyl imidazolium

dx.doi.org/10.1021/cg3004917 | *Cryst. Growth Des.* XXXX, XXX, XXX−XXX

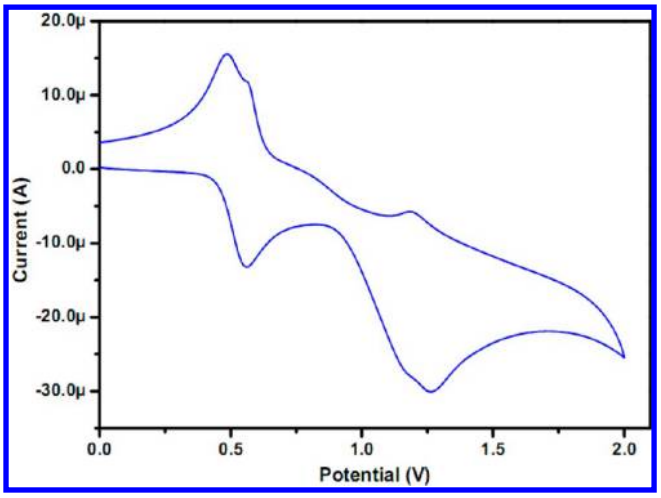

Figure 9. Cyclic voltammogram of the complex **1c** in TBAP/acetonitrile at a scan rate 50 mV s^{-1}.

Scheme 4

$$[ML_2]^{1-} \underset{-e}{\overset{e}{\rightleftharpoons}} [ML_2]^{2-} \underset{-e}{\overset{e}{\rightleftharpoons}} [ML_2]^{3-}$$

cation on the red-ox potential of complex anion $[Cu^{II}(mnt)_2]^{2-}$ in solution state.

ESR Spectroscopy. Figure 10 illustrates the representative EPR spectra of complex **1b** in the solid state both at room

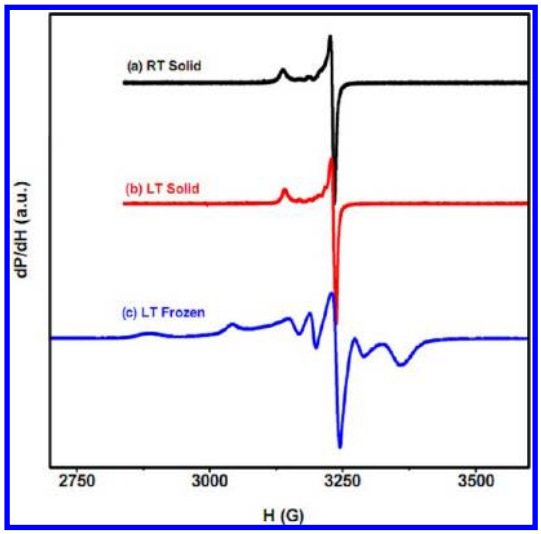

Figure 10. The EPR spectra of complex **1b**: (a) solid state at room temperature, (b) solid state at liquid nitrogen temperature, and (c) in DMF (frozen state at liquid nitrogen temperature).

temperature (frequency range is 9155.559–9161.153 MHz, Field range is 324.00–400.00 mT) and liquid nitrogen temperature (frequency range: 9155.819–9162.786 MHz, field: 324 mT), and frozen state at liquid nitrogen temperature (frequency range: 9135.349–3151.168 MHz, field: 336 mT). The EPR spectra for all compounds **1a–1f** are presented in section 14 of Supporting Information. The EPR features are almost identical at both ambient and liquid nitrogen temperature for the solid. The ligand hyperfine structure provides direct information about the nature of the electronic ground state of the complex and the extent to electron spin delocalization over ligand orbitals.[27] We have observed hyperfine splitting in the EPR spectra of compounds **1a–1f** in frozen state at liquid nitrogen temperature (see last section of Supporting Information). HOMO level of the $[Cu(mnt)_2]^{2-}$ consists of the $3d_{xy}$ orbital of copper and hybrids of 3s, $3p_x$, and $3p_y$ orbitals of sulfur atoms. These atomic orbitals are mixed with the p_z orbitals of copper and sulfur, and such mixing has a direct effect on the copper hyperfine splitting.[7a,9a,28] The g values ($g_\parallel > g_\perp$) of all these complexes are shown in Table 3,

Table 3. EPR Data of the Complexes 1a–1f

name of compound	ambient temp		liquid nitrogen temp	
	$g_\parallel$	$g_\perp$	$g_\parallel$	$g_\perp$
1a	2.100	2.034	2.088	2.025
1b	2.083	2.023	2.082	2.023
1c	2.091	2.024	2.091	2.022
1d		2.030		2.030
1e	2.088	2.026	2.089	2.026
1f	2.084	2.028	2.083	2.025

that are closed to those ($g_\parallel$ = 2.090, $g_\perp$ = 2.024, and g_1 = 2.089, g_2 = 2.024, g_3 = 2.017) of the nonplanar Cu(II)-dithiolene complexes, $[mb]_2[Cu(mnt)_2]\cdot Me_2CO$ (mb = methylene blue)[9a] and $[(Ph)_4As]_2[Cu(mnt)_2]$,[7a] respectively. These g values are also consistent ($g_\parallel$ = 2.08, $g_\perp$ = 2.02; $g_\parallel$ = 2.210, $g_\perp$ = 2.018; $g_\parallel$ = 2.21, $g_\perp$ = 2.04 and $g_\parallel$ = 2.095, $g_\perp$ = 2.033) with the planar copper complexes, $[Bu_4N]_2[Cu(mnt)_2]$, $[TBA]_2[Cu(bcd)_2]$ (bcd^{2-} = 1-benzoyl-1-cyanoethylene-2,2-dithiolate), $[Cu(gua)_2]\cdot 2DMF$ and $[Co(phen)_3][Cu(mnt)_2]$.[29,6g] From these data it can be concluded that there is an unpaired electron in the $d_{x_2-y_2}$ orbital of copper(II) in the ground state.[30]

XRPD. To ensure the phase purity of the products, X-ray powder diffraction data for all the compounds have been recorded. Similar diffraction patterns for the simulated data (calculated from single crystal data) and observed data prove the bulk homogeneity of the crystalline solids (see section-2 in Supporting Information). Although the experimental patterns have few unindexed diffraction peaks and some are slightly broadened and shifted in comparison to those simulated from the single-crystal data, it can still be regarded that the bulk as-synthesized materials represent compounds **1a–1f**.

CONCLUSION

In summary, we have reported six new ion-pair compounds **1a–1f**, in which the complex anion is common but the length of the alkyl chain in cationic moiety is varied. The geometry around the central metal ion mainly depends on the supramolecular interactions with the respective cations in the ion-pair compounds. Distorted square planar and perfect square planar geometries of the metal centers depend on center of symmetry (*Ci*) along the metal–hydrogen bond through anion $[Cu(mnt)_2]^{2-}$, and balanced/unbalanced S···H, N···H and Cu···S supramolecular interactions with the cations. The compounds, reported in this article, represent classic examples of ion pair compounds, in which the geometry of the metal ion in the complex anion/distortion from the planarity of the complex anion can be regulated by increasing/decreasing the alkyl chain length in between two imidazolium moieties in the cation. The complexes **1a–1f** show diffuse reflectance spectra, in which, we observe a bathochromic shift (total span 147 nm) depending on angle between two SMS planes in the chelate

dx.doi.org/10.1021/cg3004917 | *Cryst. Growth Des.* XXXX, XXX, XXX–XXX

rings of the anion $[Cu(mnt)_2]^{2-}$. We have demonstrated that this shift range depends on geometry around the metal ion of the complex anion in each ion pair compound. The more is the dihedral angle in $[Cu(mnt)_2]^{2-}$ (or more is the distortion), the more is the red shift in band maxima in their diffuse reflectance spectra (in the solid state). The significance of hydrogen bonding interactions in the solid state can be realized when we perform the solution electronic absorption studies for all compounds **1a**−**1f**, when we do not observe any shift (red shift) of band maxima. The present study opens a new dimension in solid state coordination chemistry of metal-dithiolene complexes, in which the energy of the solid state electronic absorption of a series of ion pair compounds can be tuned/varied by choosing an appropriate imidazolium cation in the concerned synthesis. The relevant studies of nickel analogues with imidazolium cations have been under progress.

■ ASSOCIATED CONTENT

Ⓢ Supporting Information

Crystallographic data, IR, ^{1}H NMR, LC-MS, EPR, electrochemical and other related data of the compounds **1a**−**1f**. This information is available free of charge via the Internet at http://pubs.acs.org/.

■ AUTHOR INFORMATION

Corresponding Author

*E-mail: skdsc@uohyd.ernet.in; samar439@gmail.com. Fax: +91-40-2301-2460. Tel:+91-40-2301-1007.

Notes

The authors declare no competing financial interest.

■ ACKNOWLEDGMENTS

The authors thank the Department of Science and Technology, Government of India (Project No. SR/SI/IC-23/2007) and Centre for Nanotechnology (CFN), University of Hyderabad for financial support. The National X-ray Diffractometer facility at University of Hyderabad by the Department of Science and Technology, Government of India, is gratefully acknowledged. We are grateful to UGC, New Delhi, for providing infrastructure facility at University of Hyderabad under UPE grant. We thank Mr. Suresh for his help in recording the EPR spectra for all the complexes. R.K. thanks CSIR, India, for his fellowship.

■ REFERENCES

(1) (a) McCleverty, J. A. *Prog. Inorg. Chem.* **1968**, *10*, 49−221. (b) Coucouvanis, D. *Prog. Inorg. Chem.* **1970**, *11*, 233−371. (c) Eisenberg, R. *Prog. Inorg. Chem.* **1971**, *12*, 295. (d) Alcacer, L. (1983) Novais in *Extended Linear Chain Compounds* (Miller, J. S., Eds.), Vol. 3, Chapter 6, p 319, Plenum Press, New York. (e) Alvarez, S.; Ramon, V.; Hoffman, R. *J. Am. Chem. Soc.* **1985**, *107*, 6253−6277. (f) Progress in Inorganic Chemistry, Vol. *52*, *Dithiolene Chemistry: Synthesis Properties, and Applications* (Karlin, K. D.; Tiefel, E. I., Eds.), John Wiley & Sons, New York, 2004.

(2) (a) Belo, D.; Almeida, M. *Coord. Chem. Rev.* **2010**, *254*, 1479−1492. (b) Clemenson, P. I. *Coord. Chem. Rev.* **1990**, *106*, 171−203. (c) Pullen, A. E.; Olk, R.-M. *Coord. Chem. Rev.* **1999**, *188*, 211−262. (d) Underhill, A. E.; Ahmad, M. M. *J. Chem. Soc., Chem. Commun.* **1981**, 67−68. (e) Kobayashi, A.; Sasaki, Y.; Kobayashi, H.; Underhill, A. E.; Ahmad, M. M. *J. Chem. Soc., Chem. Commun.* **1982**, 390−391. (f) Coomber, A. T.; Beljonne, D.; Friend, R. H.; Bredas, J. L.; Charlton, A.; Robertson, N.; Underhill, A. E.; Kurmoo, M.; Day, P. *Nature* **1996**, *380*, 144−146. (g) Bonneval, B. G.-D.; Ching, K. I. M.-C.; Alary, F.; Bui, T.-T.; Valade, L. *Coord. Chem. Rev.* **2010**, *254*, 1457−1467.

(3) (a) Robertson, N.; Cronin, L. *Coord. Chem. Rev.* **2002**, *227*, 93−127. (b) Siedle, A. R.; Candela, G. A.; Finnegan, T. F.; Van DuynE, R. P.; Cape, T.; Kokoszka, G. F.; Woyciejes, P. M.; Hashmall, J. A. *Inorg. Chem.* **1981**, *20*, 2635−2640. (c) Ahmad, M. M.; Turner, D. J.; Underhill, A. E.; Jacobsen, C. S.; Mortensen, K.; Carneiro, K. *Phys. Rev. B* **1984**, *29*, 4796−4799. (d) Belo, D.; Figueira, M. J.; Santos, I. C.; Gama, V.; Pereira, L. C.; Henriques, R. T.; Almeida, M. *Polyhedron* **2005**, *24*, 2035−2042. (e) Pullen, A. E.; Faulmann, C.; Pokhodnya, K. I.; Cassoux, P.; Tokumota, M. *Inorg. Chem.* **1998**, *37*, 6714−6720.

(4) (a) Staniland, S. S.; Fujita, W.; Umezone, Y.; Awaga, K.; Camp, P. J.; Clark, S. J.; Robertson, N. *Inorg. Chem.* **2005**, *44*, 546−551. (b) Ren, X.; Meng, Q.; Song, Y.; Hu, C.; Lu, C.; Chen, X.; Xue, Z. *Inorg. Chem.* **2002**, *41*, 5931−5933. (c) Ni, C.; Tian, Z.; Ni, Z.; Dang, D.; Li, Y.; Song, Y.; Meng, Q. *Inorg. Chim. Acta* **2006**, *359*, 3927−3933. (d) Robertson, N.; Bergemann, C.; Becher, H.; Agarwal, P.; Julian, S. R.; Friend, R. H.; Hatton, N. J.; Underhill, A. E.; Kobayashi, A. *J. Mater. Chem.* **1999**, *9*, 1713−1717. (e) Nishijo, J.; Ogura, E.; Yamaura, J.; Miyazaki, A.; Enoki, T.; Takano, T.; Kuwatani, Y.; Iyoda, M. *Synth. Met.* **2003**, *133*−*134*, 539−541. (f) Muller-Westerhoff, U. T.; Vance, B.; Yoon, D. I. *Tetrahedron* **1991**, *47*, 909−932. (g) Kato, R. *Chem. Rev.* **2004**, *104*, 5319−5346.

(5) (a) Yao, B.-Q.; Sun, J.-S.; Tian, Z.-F.; Ren, X.-M.; Gu, D.-W.; Shen, L.-J.; Xie, J. *Polyhedron* **2008**, *27*, 2833−2844. (b) Bigoli, F.; Cassoux, P.; Deplano, P.; Mercuri, M. L.; Pellinghelli, M. A.; Pintus, G.; Serpe, A.; Trogu, E. F. *J. Chem. Soc., Dalton Trans.* **2000**, 4639−4644. (c) Bremi, J.; D'Agostino, E.; Gramlich, V.; Caseri, W.; Smith, P. *Inorg. Chim. Acta* **2002**, *335*, 15−20.

(6) (a) Gao, X.-K.; Dou, J.-M.; Li, D.-C.; Dong, F.-Y.; Wang. *J. Chem. Cryst.* **2005**, *35*, 345−350. (b) Ni, C.; Zheng, Y.; Yang, L.; Li, Y. *J. Coord. Chem.* **2006**, *59*, 1037−1043. (c) YunXia, S.; LiLi, W.; Huan, Z.; QingJin, M. *Sci. China Ser. B-Chem.* **2007**, *50*, 607−613. (d) Ren, X.; Ma, J.; Lu, C.; Yang, S.; Meng, Q.; Wu, P. *Dalton Trans.* **2003**, 1345−1351. (e) Dang, D.; Ni, C.; Ni, Z.; Li, Y.; Meng, Q.; Yao, Y. *J. Coord. Chem.* **2005**, *58*, 195−201. (f) Ren, X. M.; Okudera, H.; Xie, J. L.; Meng, Q. J. *J. Mol. Struct.* **2005**, *733*, 119−124. (g) Singh, N.; Singh, V. K. *Int. J. Inorg. Mater.* **2000**, *2*, 167−175.

(7) (a) Stach, J.; Kirmse, R.l; Sieler, J.; Abram, U.; Dietzsch, W.; Bottcher, R.; Hansen, L. K.; Vergoossen, H.; Gribnau, M.; Keijzers, C. P. *Inorg. Chem.* **1986**, *25*, 1369−1373. (b) Bereman, R. D.; Lu, H. *Inorg. Chim. Acta* **1993**, *204*, 53−61. (c) Hoyer, E.; Dietzxch, W.; Schroth, W. *Z. Chem.* **1971**, *11*, 41−53. (d) Coucouvanis, D.; Holah, D. G.; Hollander, F. J. *Inorg. Chem.* **1975**, *14*, 2657−2655. (e) Burns, R. P.; McAuliffe, C. A. *Adv. Inorg. Chem. Radiochem.* **1979**, *22*, 303−348. (f) Maki, A. H.; Edelstein, N.; Davison, A.; Holm, R. H. *J. Am. Chem. Soc.* **1964**, *86*, 4580−4587. (g) Kirmse, R.; Stach, J.; Dietzsch, W.; Steimecke, G.; Hoyer, E. *Inorg. Chem.* **1980**, *19*, 2679−2685.

(8) (a) Venkatalakshmi, N.; Varghese, B.; Lalitha, S.; Williams, R. F. X.; Manoharan, P. T. *J. Am. Chem. Soc.* **1989**, *111*, 5748−5757. (b) Ren, X. M.; Ni, Z. P.; Noto, S.; Akutagawa, T.; Nishihara, S.; Nakamura, T.; Sui, Y. X.; Song, Y. *Cryst. Growth Des.* **2006**, *6*, 2530−2537. (c) Kishore, R.; Tripuramallu, B. K.; Durgaprasad, G.; Das, S. K. *J. Mol. Struct.* **2011**, *990*, 37−43. (d) Belo, D.; Figueira, M. J.; Santos, I. C.; Gama, V.; Pereira, L. C.; Henriques, R. T.; Almeida, M. *Polyhedron* **2005**, *24*, 2035−2042.

(9) (a) Snaathorst, D.; Doesburg, H. M.; Perenboom, J. A. A. J.; Keijzers, C. P. *Inorg. Chem.* **1981**, *20*, 2526−2532. (b) Lundquist, O.; Anderson, L.; Sieler, J.; Steimeeke, G.; Hoyer, E. *Acta Chem. Scand., Ser. A* **1982**, *36*, 855−856. (c) Hunter, C.; Weakly, T. J. R. *J. Chem. Soc., Dalton Trans.* **1983**, 1067−1070. (d) Mahadevan, C.; Seshasayee, M. *J. Crystallogr. Spectrosc. Res.* **1984**, *14*, 215−226.

(10) Huertas, S.; Hissler, M.; McGarrach, J. E.; Lachicotte, R. J.; E. *Inorg. Chem.* **2001**, *40*, 1183−1188.

(11) Maganas, D.; Grigoropoulos, A.; Staniland, S. S.; Chatziefthimiou, S. D.; Harrison, A.; Robertson, N.; Kyritsis, P.; Neese, F. *Inorg. Chem.* **2010**, *49*, 5079−5093.

(12) (a) Martin, E. M.; Bereman, R. D.; Singh, P. *Inorg. Chem.* **1991**, *30*, 957−962. (b) Bu, X.-H.; Chen, W.; Lu, S.-L.; Zhang, R.-H.; Liao,

D.-Z.; Bu, W.-M.; Shionoya, M.; Brisse, F.; Ribas, J. *Angew. Chem., Int. Ed.* **2001**, *40*, 3201−3203. (c) Bu, X.-H.; Chen, W.; Hou, W.-F.; Du, M.; Zhang, R.-H.; Brisse, F. *Inorg. Chem.* **2002**, *41*, 3477−3482. (d) Goodgame, D. M. L.; Grachvogel, D. A.; Hussain, I.; White, A. J. P.; Williams, D. J. *Inorg. Chem.* **1999**, *38*, 2057−2063.

(13) Arion, V. B.; Rapta, P.; Telser, J.; Shova, S. S.; Breza, M.; Luspai, K.; Kozisek, J. *Inorg. Chem.* **2011**, *50*, 2918−2931.

(14) (a) Moigne, C. L.; Picaud, T.; Boussac, A.; Loock, B.; Momenteau, M.; Desbois, A. *Inorg. Chem.* **2003**, *42*, 6081−6088. (b) Collins, D. M.; Countryman, R.; Hoard, J. L. *J. Am. Chem. Soc.* **1972**, *94*, 2066−2072. (c) Little, R. G.; Dymock, K. R.; Ibers, J. A. *J. Am. Chem. Soc.* **1975**, *97*, 4532−4539. (d) Ogura, H.; Yatsunyk, L.; Medforth, C. J.; Smith, K. M.; Barkigia, K. M.; Renner, M. W.; Melamed, D.; Walker, F. A. *J. Am. Chem. Soc.* **2001**, *123*, 6564−6578.

(15) (a) Song, X.-Z.; Jentzen, W.; Jia, S.-L.; Jaquinod, L.; Nurco, D. J.; Medforth, C. J.; Smith, K. M.; Shelnutt, J. A. *J. Am. Chem. Soc.* **1996**, *118*, 12975−12988. (b) Haddad, R. E.; Gazeau, S.; Pecaut, J.; Marchon, J.-C.; Medforth, C. J.; Shelnutt, J. A. *J. Am. Chem. Soc.* **2003**, *125*, 1253−1268.

(16) (a) White, D. J.; Cronin, L.; Parsons, S.; Robertson, N.; Tasker, P. A.; Bisson, A. P. *Chem. Commun.* **1999**, 1107−1108. (b) McMaster, J.; Beddoes, R. L.; Collison, D.; Eardley, D. R.; Helliwell, M.; Garner, C. D. *Chem.-Eur. J* **1996**, *2*, 685−693. (c) Braga, D.; Grepioni, F. *J. Chem. Soc.; Dalton Trans.* **1999**, 1−8.

(17) (a) Huynh, H. V.; Han, Y.; Ho, J. H. H.; Tan, G. K. *Organometallics* **2006**, *25*, 3267−3274. (b) Braga, D.; Grepioni, F.; Tedesco, E.; Biradha, K.; Desiraju, G. R. *Organometallics* **1997**, *16*, 1846−1856. (c) Zhang, Y.; Lewis, J. C.; Bergman, R. G.; Ellman, J. A.; Oldfield, E. *Organometallics* **2006**, *25*, 3515−3519. (d) Crabtree, R. H.; Eisenstein, O.; Sini, G.; Peris, E. *J. Organomet. Chem.* **1998**, *567*, 7−11.

(18) (a) Schiavo, S. L.; Nicolo, F.; Scopelliti, R.; Tresoldi, G.; Piraino, P. *Inorg. Chim. Acta* **2000**, *304*, 108−113. (b) Dehand, J.; Fisher, J.; Pfeffer, M.; Mitschler, A.; Zinsius, M. *Inorg. Chem.* **1976**, *15*, 2675−2681. (c) Brammer, L.; Charnock., J. M.; Goggin, P. L.; Goodfellow, R. J.; OPrpen, A. G.; Koetzle, T. F. *J. Chem. Soc.; Dalton Trans.* **1991**, 1789−1798. (d) Pei, W.-B.; Liu, J.-L.; Wu, J.-S.; Ren, X.-M.; Gu, D.-W.; Shen, L.-J.; Meng, Q.-J. *J. Mol. Struct.* **2009**, *918*, 160−164.

(19) Chang, J.-C.; Ho, W.-Y.; Sun, I.-W.; Chou, Y.-K.; Hsieh, H.-H.; Wu, T.-Y. *Polyhedron* **2011**, *30*, 497−507.

(20) Locke, J.; McCleverty, J. A. *Inorg. Chem.* **1966**, *5*, 1157−1161.

(21) (a) *SAINT: Software for the CCD Detector System*; Bruker Analytical X-ray Systems, Inc.: Madison, WI, 1998. (b) *SADABS: Program for Absorption Correction*; G. M. Sheldrick University of Gottingen: Gottingen, Germany, 1997. (c) *SHELXS-97: Program for Structure Solution*; G. M. Sheldrick, University of Gottingen: Gottingen, Germany, 1997. (d) *SHELXL-97: Program for Crystal Structure Analysis*; G. M. Sheldrick University of Gottingen: Gottingen, Germany, 1997.

(22) (a) Zhou, H.; Wen, L. L.; Ren, X. M.; Meng, Q. J. *J. Mol. Struct.* **2006**, *787*, 31−37. (b) Dang, D.; Bai, Y.; Wen, L.; Tian, Z.; Li, Y.; Meng, Q. *J. Mol. Struct.* **2005**, *753*, 99−103. (c) Dang, D.; Ni, C.; Bai, Y.; Tian, Z.; Wen, L.; Meng, Q.; Gao, S. *J. Mol. Struct.* **2005**, *743*, 197−200.

(23) (a) Huang, Q.; Lin, J.-H.; Liang, L.-B.; Chen, X.; Zuo, H.-R.; Zhou, J.-R.; Yang, L.-M.; Ni, C.-L.; Hu, X.-L. *Inorg. Chim. Acta* **2010**, *363*, 2546−2552. (b) Kiani, S.; Long, J. R.; Stavropoulos, P. *Inorg. Chim. Acta* **1997**, *263*, 357−366.

(24) (a) Shupack, S. I.; Billig, E.; Clark, R. J. H.; Williams, R.; Gray, H. B. *J. Am. Chem. Soc.* **1964**, *86*, 4594−4602. (b) Schrauzer, G. N.; Mayweg, V. P. *J. Am. Chem. Soc.* **1965**, *87*, 3585−3592.

(25) Madhu, V.; Das, S. K. *Polyhedron* **2004**, *23*, 1235−1242.

(26) (a) Dietzsch, W.; Lerchner, J.; Reinhold, J.; Stach, J.; Kirmse, R.; Stimecke, G.; Hoyer, E. *J. Inorg. Nucl. Chem.* **1980**, *42*, 509−520. (b) Persaud, L.; Langford, C. H. *Inorg. Chem.* **1985**, *24*, 3562−3567. (b) Mines, T. E.; Geiger, W. E. *Inorg. Chem.* **1973**, *12*, 1189−1191.

(27) Schmitt, R. D.; Maki, A. H. *J. Am. Chem. Soc.* **1968**, *90*, 2288−2292.

(28) (a) Kirmse, R.; Dietzsch, W.; Stach, J.; Golic, L.; Bottcher, R.; Brunner, W.; Gribnau, M. C. M.; Keijzers, C. P. *Mol. Phys.* **1986**, *57*, 1139−1152. (b) Reijerse, E. J.; Thiers, A. H.; Kanters, R.; Gribnau, M. C. M.; Keijzers, C. P. *Inorg. Chem.* **1987**, *26*, 2764−2769.

(29) (a) Bilig, E.; Williams, R.; Bernal, I.; Waters, J. H.; Gray, H. B. *Inorg. Chem.* **1964**, *3*, 663−666. (b) Singh, N.; Prasad, A.; Gupta, S. *Transition Met. Chem.* **2005**, *30*, 383−388. (c) Tomas, A.; Viossat, B; Charlot, M.-F.; Girerd, J.-J.; Huy, D. N. *Inorg. Chim. Acta* **2005**, *358*, 3253−3258.

(30) Hathway, B. J.; Wilkinson, G.; Gillard, R. D.; McCleverty, J. A., Eds. (1987)*Comprehensive Coordination Chemistry*, Vol *5*, p 533, Pergamon Press, Oxford, England.